8-2004

A Characteristic Study of the Atmospheric Pressure Nonthermal Resistive Barrier Plasma Discharge for Biological Decontamination

Magesh Thiyagarajan
University of Tennessee - Knoxville

To the Graduate Council:

I am submitting herewith a thesis written by Magesh Thiyagarajan entitled "A Characteristic Study of the Atmospheric Pressure Nonthermal Resistive Barrier Plasma Discharge for Biological Decontamination." I have examined the final electronic copy of this thesis for form and content and recommend that it be accepted in partial fulfillment of the requirements for the degree of Master of Science, with a major in Electrical Engineering.

Igor Alexeff, Major Professor

We have read this thesis and recommend its acceptance:

J. Douglas Birdwell, Gregory Peterson

Accepted for the Council:
Carolyn R. Hodges

Vice Provost and Dean of the Graduate School

(Original signatures are on file with official student records.)

To the Graduate Council:

I am submitting herewith a thesis written by Magesh Thiyagarajan entitled "A Characteristic Study of the Atmospheric Pressure Nonthermal Resistive Barrier Plasma Discharge for Biological Decontamination". I have examined the final electronic copy of this thesis for form and content and recommend that it be accepted in partial fulfillment of the requirements for the degree of Master of Science, with a major in Electrical Engineering.

Igor Alexeff,
Major Professor

We have read this thesis and
recommend its acceptance:

J. Douglas Birdwell

Gregory Peterson

Accepted for the Council:

Anne Mayhew

Vice Chancellor and Dean of
Graduate Studies

(Original signatures are on file with official student records.)

A Characteristic Study of the Atmospheric Pressure Nonthermal Resistive Barrier Plasma Discharge for Biological Decontamination.

A Thesis
Presented for the
Master of Science
Degree
The University of Tennessee, Knoxville

Magesh Thiyagarajan
August 2004

DEDICATION

I dedicate this thesis to my mother

Sri. Mrs. Sagunthala Thiyagarajan

and

my inspirational guru

Dr. Igor Alexeff

My mom and I had to go through a lot of obstacles to come to this point. Although miles far away, I still feel her presence supporting me to overcome any obstacles, however big they may be.

ACKNOWLEDGEMENTS

I would like to thank everyone who supported me in finishing this thesis. I am most thankful to my advisor, Dr. Igor Alexeff for taking a chance on me almost two years ago, providing me with opportunities I had not even dreamt of, and for his supervision, his guidance, his unending support, and his friendship.

Thanks are also extended to my committee members, Dr. J. Douglas Birdwell and Dr. Gregory Peterson for being in my committee and for also giving me valuable guidance on preparing this thesis material.

I would like to acknowledge Dr. Stephen Beebe, Associate Professor, Eastern Virginia Medical School, for supporting us with the biological experiments and results.

I am so grateful to my beloved brother, Mr. Suresh Thiyagarajan for his unending encouragement and support. He is my role model of hard working and commitment.

I also would like to thank Mr. Sriram Parameswaran for helping me to carry out the experiments, constant cooperation with the laboratory affairs and also for helping me in taking good decision in delicate situations. Though we had ups and downs, we had a good time working together.

I had the pleasure of meeting many people during my studies in Knoxville. Among them, the most significant figure in my life at UT was my aunt, Mrs. Felicia Felder. “Aunt!” I will always remember your kindness, caring and most of all our friendship. Thank you for all of the good times.

Finally, someone special for me deserves extra recognition, Visweswaran Srinivasamurthy (Anand) for being there for me in the difficult times. I do not know how I could have gone through the early days of my studies at UT without his unending moral and adored support.

ABSTRACT

Steady-state atmospheric pressure nonthermal plasmas can splendidly debilitate bacteria in liquids, gases and on surfaces, as well as can disintegrate hazardous chemicals. The nonthermal gas discharge at atmospheric pressure, such as resistive barrier discharge is investigated for low temperature sterilization purposes. In specific, exploring and understanding the hidden secrets of the plasma sterilization mechanisms and the intensification of the main microbial reduction pathways are the objectives of the research.

A dual-mode steady-state atmospheric pressure resistive barrier ionized gas (plasma) generator has been designed and developed to meet the environmental health and federally mandated safety standards. Electrical, chemical, optical, and biological studies are carried out on the Steady-State, Atmospheric Pressure Resistive Barrier Discharge, with the intent of identifying the chemically and biologically active species produced. The goals of the research work are to prepare an effective, inexpensive plasma sterilization process and to identify and escalate the main contributing active species responsible for plasma sterilization.

The effectiveness of ionized gases produced by the resistive barrier plasma discharge on sterilizing bacteria has been analyzed. Bacteria at a dilution that achieved a countable number of colonies were exposed or not exposed to ionized gases for various periods of time and monitored to determine the effects of ionized gas treatment. The

results of these experiments indicate that effective decontamination can be achieved within minutes when bacteria are exposed to ionized gases in close contact to the contaminating surface. On the battlefield or in remote locations, ionized gases could be used to decontaminate potentially harmful agents of bacterial origin. In hospitals on the battlefield and/or in remote locations, ionized gasses could be used to sterilize surgical equipment, decontaminate potentially infected areas in post-operative care units following surgery. In such cases the self-generated gas flow from the reactor facilitates the application of the ionized gases over the large infected areas.

TABLE OF CONTENTS

CHAPTER **PAGE**

LIST OF FIGURES

FIGURE **PAGE**

CHAPTER 1

Introduction

Long a hypothetical threat, bioterrorism became a harsh reality soon after the terrorist attack on the World Trade Center (WTC), called Twin Towers of the New York city, USA on September 11, 2001, when letters containing a refined preparation of dried anthrax spores were sent through the U.S. mail, infecting more than twenty people and killing five. Although the October 2001 anthrax attack was fortunately limited in scale, it hinted at the mayhem that could result from the deliberate release of "weaponized" disease agents. Nonequilibrium, atmospheric pressure plasma discharges are increasingly being used in various novel applications including sterilization [Laroussi, 2000]. In many of these applications, a nonthermal, large volume, atmospheric pressure discharge, which can be generated in a practical and economical way, is sought.

1. 1. Definition and Characteristics of a Gas Plasma

Gas plasmas, simply termed plasmas by physicists who don't fear ambiguity with the blood component, can be considered as the fourth state of matter, following by order of increasing energy, the solid state, the liquid state and the gaseous state. This fourth state, as encountered in stars, is strictly speaking a gas made of positive and negative ions and free electrons only. However, the plasmas employed for sterilization are much colder and are actually *ionized gases*: besides ions and electrons, ionized gases also consist of uncharged particles, such as atoms, molecules and radicals (atoms or assembly of atoms

with unpaired electrons, therefore chemically reactive, eg O and OH, respectively), collectively called *neutrals*. In this presentation, as is common practice, I shall use the term plasma to designate as well an ionized gas, ignoring the above distinction.

Ions and neutral atoms (molecules) can be in an excited state; i.e., they can have *internal energy*, this energy being zero when these particles are in their ground state. Excited particles can de-excite (lose their internal energy), either spontaneously by emitting a photon or through collisions with other particles or a surface. Collision with a surface can lead to the physical sputtering of their elements or to chemical reactions, such as oxidation, resulting in some cases in a volatile compound (eventually pumped out) formed between the incoming (adsorbed) atom (radical, molecule) and a surface atom. Photons emitted by excited species can also induce chemical reactions on a surface: UV photons are particularly efficient in this respect [Lerouge et al., 2000a].

Man-made plasmas are usually produced by subjecting a gas (or gases) to an electric field (say, between two electrodes), either of constant (direct-current, d.c., field) or alternating amplitude (usually high frequency field), hence their designation as *electrical discharges*. The electric field E accelerates the charged particles, essentially the electrons since the ions are much heavier, and the E-field energy is ultimately communicated to the plasma through collisions of the electrons with the heavy particles [Delcroix and Bers, 1994; Moisan and Pelletier, 1999].

1. 2. The Glow and the Flowing Afterglow of a Plasma

As a rule in electrical discharges, most of the gas volume is quite luminous, which is why one speaks of a *glow discharge*. When the discharge takes place in a flowing gas, some of the species produced in the glow region can be carried away into an electric field-free vessel, and one obtains what is called a *flowing afterglow*.

Plasma sterilization can be achieved either in the glow or in the afterglow region. Compared to the glow region, the afterglow contains relatively few charged particles, being essentially comprised of neutral atoms, radicals and molecules, some of which are in an excited state. The species of interest are then short-lived particles, for instance atoms like O and N, and excited molecules such as NO in an O_2–N_2 gas discharge. Short-lived particles, therefore, need to be carried to their point of use rapidly enough, hence a minimum value for the gas flow rate. The main advantages of using the afterglow for sterilization purposes instead of the discharge itself [Moreau et al., 2000] can be summarized in the following points:

(1) With high density plasmas such as those produced by microwaves (unless operated in a pulsed regime), the gas temperature in the discharge itself can reach a few hundreds Celsius, while it can be made less than 50 °C in the corresponding afterglow, an important characteristic when dealing with heat-sensitive materials.

(2) Under direct plasma exposure, the treated surfaces have some chances of being altered by the impact of the (positive) ions accelerated in the *sheath*. The sheath is the interfacial region between the plasma and any surface immersed in it where the ion density exceeds that of electrons (both densities are equal in the plasma). This non-neutrality results from a potential difference between the plasma and the surface, which accelerates ions toward the surface. There is no sheath in an afterglow.

(3) There is no essential need to operate in the discharge itself since, as shown by recent studies; it is the neutral species that play the major role in plasma sterilization [Khomich et al., 1997].

(4) The presence in the processing region of the E-field sustaining the plasma can induce local heating in non-dielectric devices, hence possible damage to them.

(5) The afterglow can fill larger chamber volumes at lower costs than the corresponding glow discharge. However, sterilization time is usually much shorter in the discharge itself than in its afterglow. In both operating modes, one must ensure that enough active species reach all parts of the devices to be sterilized, everywhere in the chamber.

1. 3. Cold Plasmas

The plasmas most commonly used for sterilization purposes are known as cold plasmas with reference to their gas temperature. This is because heavy particles (neutrals and ions) in these plasmas have temperatures much lower (typically at least ten times) than the temperature (average energy) of the electrons. At pressures typically below 10 Torrs (≈10 mbar), cold plasmas are characterized by a mean electron energy in the range 1–5 eV (1 eV=1.6×10^{-19} J or 11600 K). Therefore, it is the electrons that break molecules, and excite or ionize atoms and molecules of the discharge gas without requiring the heavy particles to be as energetic [Boucher, 1985], hence a lower energy cost and the possibility of using glass and metal discharge vessels without a heavy cooling. With some kinds of pulsed discharges, the gas temperature can even be as low as room temperature. As a rule, the temperature of the discharge gas increases with pressure (because of the increasing number of elastic collisions of electrons with heavy particles) and, depending on the gas, can exceed a few thousands degrees at atmospheric pressure unless a pulsed discharge is used. Low-temperature sterilization under direct plasma exposure can be realized by running d.c. discharges (which means constant E-field intensity as a function of time), radio-frequency (RF; typically 1–100 MHz) and microwave (≥300 MHz) discharges under low current and low power conditions, respectively. It can also be achieved by sustaining microwave discharges in a pulsed mode [Griffiths and Raybone, 1992; Lerouge et al., 2000b] or by using very low frequency E-field (eg 1–10 kHz), as required to operate corona discharges and DBDs [Kelly-Wintenberg et al., 1998; Kuzmichev et al., 2000; Laroussi et al., 2000].

CHAPTER 2

Properties of Barrier Discharge

Barrier discharges (BDs) produce highly non-equilibrium plasmas in a controllable way at atmospheric pressure, and at moderate gas temperature. They provide the effective generation of atoms, radicals and excited species by energetic electrons. There are two different modes of BDs. Generally they are operated in the filamentary one. Under special conditions, a diffuse mode can be generated. BDs are applied for a long time in the wide field of plasma treatment and layer deposition. BDs have a great flexibility with respect to their geometrical shape, working gas mixture and operation parameters. Generally, the scaling-up to large dimensions is no problem. The possibility to treat or coat surfaces at low gas temperature and pressures close to atmospheric is an important advantage for their application.

Decisive advantages of the BDs for the wide field of applications are the non-thermal plasma conditions at low gas temperatures and at elevated (typically atmospheric) pressure. BDs provide high-energy electrons, which are able to generate atoms, radicals and excited particles. These discharges demonstrate a great flexibility with respect to their geometrical shape, working gas mixture composition and operation parameters (e.g. power input, frequency of feeding voltage, pressure, gas flow) [Eliasson 1991]. In many cases, when these parameters have been optimized before in small laboratory devices, there are no problems in scaling up the conditions to larger

(industrial) dimensions. Usually, the BD operates in the so-called filamentary mode. Under (very) special conditions of the operation, there exist a diffuse (glow) mode, too. In the latter case, referred to as atmospheric pressure glow discharge, the BDs are very suitable for a uniform surface treatment [Kanazawa 1988, Okazaki 1993, Sawada 1995, Trunec 1998, Massines 1998, Tepper 1998, Gherardi 2000]. The generation of reactive particles (atoms, radicals, excited species, ions) and of radiation at short wavelength for surface treatment is controlled by the plasma parameters of the BD, mainly by the reduced local electric field strength and by the electron density.

2.1. Atmospheric Pressure Plasmas and Configurations of Barrier Discharge

Atmospheric pressure plasmas are subdivided into non-thermal and thermal ones. The corresponding conditions are illustrated in the Figure. 2.1. Examples for plasma sources important for numerous applications are listed, too. The conditions of non-thermal plasmas are mainly characterized by a relatively low temperature of the neutral gas in contrast to a significantly higher kinetic temperature of the electrons. The non-equilibrium between these main components is permanently maintained by applying DC or AC electric fields to the discharge electrodes. The gas temperature is often near room temperature. Therefore, these plasmas are named low-temperature non-equilibrium plasmas, too. In thermal plasmas, all species have an identical temperature characterized by one Maxwellian velocity distribution function of particles. Consequently, they are in the complete (or at least local) thermal equilibrium, which can be reached only sufficiently far from solids in contact with plasmas.

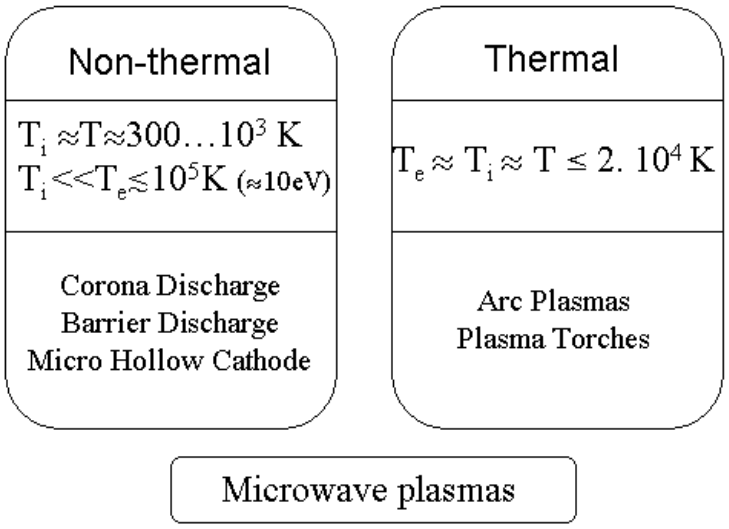

Figure-2.1 Subdivision of plasmas at atmospheric pressure.

This group includes, e.g. arcs and inductively coupled plasma torches. Microwave plasma sources can provide both regimes, depending on the operation conditions. Typical electrode arrangements of planar and cylindrical BDs are shown in Figure 2.2 The presence of one or more resistive or dielectric layers in the current path between the metallic electrodes through the discharge gap is essential for the discharge operation. Typical materials for dielectric barriers are glass, quartz and ceramics. Plastic foils, Teflon plates and other insulating materials can be used, too. There are many excellent monographs and papers on the physics of BDs, [Eliasson 1991, Samoilovich 1997, Gibalov 2000, Pietsch 2001, Kogelschatz 2001]. Because of a capacitive coupling of the insulating material to the gas gap BDs can only be driven by alternating feeding voltage or by pulsed DC voltages. Where as in the case of resistive barrier discharge the electrode arrangement is resistive.

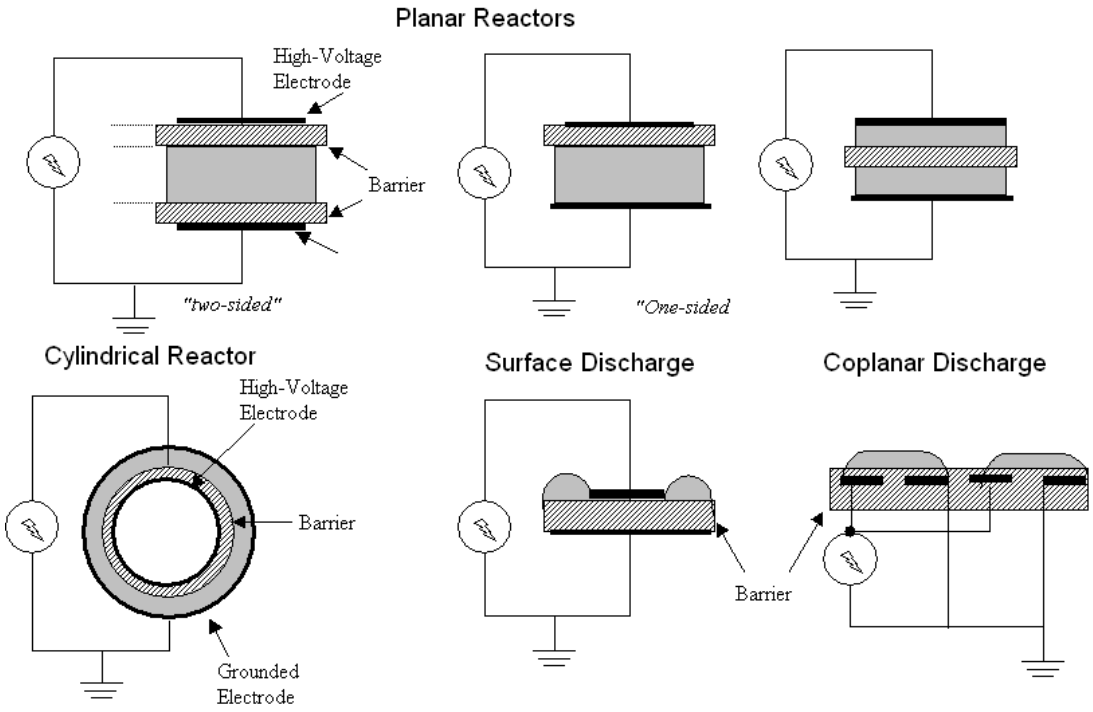

Figure-2.2 Typical electrode arrangements of barrier discharges.

Therefore the discharge can be driven either by alternating feeding voltage or steady state DC voltage. The resistive barrier prevents a high current discharge from forming an arc, and will run for a long time. The dielectric barrier discharges require an expensive high-voltage source of radio-frequency energy to generate atmospheric pressure plasma. When a high enough voltage is applied an electrical breakdown occurs.

2.2. Filamentary Barrier Discharge

Usually the BD operates in the so-called filamentary mode. If the local electric field strength in the gas gap reaches the ignition level, the breakdown starts at many points followed by the development of filaments, named micro discharges [Eliasson 1987, Braun 1991, Gibalov 2000, Pietsch 2001]. The micro discharges are of nanosecond duration, uniformly distributed over the electrode surface. To characterize the overall discharge behavior, an equivalent electric circuit can be used. In dielectric barrier discharges two capacitances in parallel such as capacitance due to the dielectric material and the capacitance due to the air gap between the electrodes are considered. In the case of resistive barrier discharges a RC parallel network is considered. The R and C are the resistance and capacitance of the barrier material.

Microscopic Behavior of Filamentary Barrier Discharge - Structure.

The electrical breakdown of the gas gap in a BD starts almost simultaneously at many points of the surface and proceeds via the development of micro discharges. Both DBDs and RBDs obey similar pulsing mechanisms for forming micro discharges. Their

development can be sub-divided into three steps [Eliasson 1991, Samoilovich 1997, Gibalov 2000, Kozlov 2001, Kogelschatz 2001].

(1) The pre-breakdown phase.

A negative space charge of electrons (and negative ions due to attachment) is accumulated in front of the anode (according to the polarity of the half cycle of applied voltage). The pre-breakdown phase lasts for at least 0.5 ms. Finally, high local electric field strength is created in front of the anode. If it reaches a certain critical level, the breakdown starts from the anode surface.

(2) The propagation phase.

It is governed by an ionization wave (i.e. a wave of high local electric field strength) in the direction to the cathode. On its way pairs of ions and electrons are produced. This phase takes typically 1–2 ns.

(3) The decay phase.

It is characterized by the charge accumulation on the dielectric surface compensating the external electric field. It is a period of decay of the light and current pulses of the micro discharges.

In the next pulsing mechanism, the micro discharge formation inversely renews. The barrier limits the amount of the transferred charge and energy deposited in a micro

discharge at the dielectric surface the micro discharge channels continue as surface discharges covering a much larger area than the diameter of the filament.

2.3. Diffuse (Glow) Barrier Discharges

Under certain operating conditions, a diffuse (glow) mode of BD can be obtained. Obviously, diffuse BDs are especially suitable for a uniform surface treatment. Donohoe (1976) investigated a uniform glow discharge with pulsed excitation in helium and ethylene mixtures. Okazaki, et al (1987) operated barrier glow discharges even at 50 Hz sinusoidal feeding voltage, using an electrode configuration of two metal foils covered with a special metal mesh and ceramic dielectrics in helium, nitrogen (and even in air, oxygen and argon) with and without certain organic admixtures [Kanazawa 1988, Okazaki 1993, Kanazawa 1987]. They proposed the term APGD; Massines, et al (1992) investigated in detail barrier glow discharges in helium and nitrogen [Massines: 1992, 1998, 2000]. This group contributed essentially to a better understanding of the existence of the glow mode in the studied systems on the level of elementary processes. Recent activities of several teams are focused on spatially and temporally resolved spectroscopic measurements [Wagner 2000, Brandenburg 2002, Trunec 2002] as well as on the development of theoretical models [Segur 2000, Golubovskii 2002]. The generation of stable diffuse BDs at atmospheric pressure requires special operation conditions that are mainly determined by the properties of feeding gas. One important point seems to be an occurrence of effective pre-ionization, Penning ionization via metastables and primary ionization at low electric field, as compared to the conditions of the BDs in the

filamentary mode. Of course, the diffuse BD mode is sensitive to impurities, admixtures, metastables and residual ions. The densities of residual species from the previous half period that can initiate the diffuse discharge generation in the next half-cycle, are dependent on the repetition frequency. Therefore, the feeding voltage frequency plays an important role in the transition to the diffuse mode. Some barrier materials can trap appreciable amounts of charges uniformly on the surface. When the electric field changes its polarity, the charge carriers are expelled from the surface initiating a diffuse discharge development [Tepper 1998]. The required operation conditions can be easily established in helium, neon and pure nitrogen. BDs produce highly non-equilibrium plasma conditions in a controllable way at atmospheric pressure, and at moderate gas temperature. The BDs provide energetic electrons, which are able to generate atoms, radicals and excited species. If noble gases (or noble gas/halogen gas mixtures) are used as working gas, they are sources of an intensive short-length excimer radiation. Both the reactive species and the excimer radiation have been applied for a long time in many fields of plasma treatment and layer deposition

With respect to a uniform surface treatment, diffuse discharge (or homogenized) conditions are very desirable. BDs have a great flexibility with respect to their geometrical shape, working gas mixture and operation parameters. The scaling-up to large (industrial) dimensions is no problem. The possibility to treat or coat surfaces at low gas temperature and pressures close to 1 atm is an important advantage of their application.

CHAPTER 3

Principles of Plasma Inactivation of Microorganisms

The advent of polymeric medical devices has stimulated users and developers to look for new methods to sterilize heat-sensitive materials. The most common technique used nowadays for such a purpose relies on ethylene oxide (EtO). The first version of this method had to be modified because of environmental regulations on chlorofluorocarbons (CFCs) that were added to EtO to reduce its flammable properties [Ernest, 1995]. Although 100% EtO sterilizers, which no longer use CFCs, have been developed, there are still many questions concerning the carcinogenic properties of the EtO residues adsorbed on the materials after processing [Steelman, 1992a; Holyoak et al., 1996; Zhang et al., 1996]. There are also worries about the safety of operators when opening the sterilizer before the end of the vent time, which is much longer than the actual sterilization time [Steelman, 1992b]. Although the most common low temperature technique currently used calls for gaseous EtO, liquid formaldehyde and glutaraldehyde, which have noxious properties too, are also employed in many medical sterilization installations [Ehrenberg et al., 1974]. Another interesting technology is the gamma irradiation process, but it is costly and its safe operation requires an isolated site; moreover, besides damaging to some extent the surface of the objects like any sterilization method, gamma irradiation also affects the bulk properties of the polymers being treated, as it breaks bonds and cross-linked chains within the volume of the material [Henn et al., 1996].

The various limitations of the above sterilization methods have fostered the development of alternative techniques. The ideal sterilizer should provide:

1. A sterilization time shorter or at least not longer than the actual processing time required with steam autoclave and dry heat methods (approx. 60 min);
2. An equal or lower processing temperature than that encountered with EtO (55 °C or less);
3. The possibility of dealing with a wide range of materials and objects;
4. Harmless operation for operators, patients and materials.

The use of a gas plasma offers an original alternative to sterilization because of the intrinsic properties of this medium. The method consists in exposing microorganisms to species stemming from an electrical discharge in a gas. In the pure form of this method, the gas or gases involved have no biocidal effect unless they are activated by the electrical discharge; these reactive species are no longer present a few milliseconds after the electric field has been turned off, which means that there is no need for vent time and, therefore, very little danger for the personnel. The operating conditions of the plasma have to be set for an efficient inactivation of the microorganisms, while minimizing the damage to the materials subjected to the treatment [Anderson, 1989; Lerouge et al., 2000a].

3.1. The First Steps of Plasma Sterilization

The first report on plasma as a sterilizing agent was by Menashi in a 1968 patent [Menashi, 1968]. The apparatus used a pulsed RF field to achieve an argon plasma at atmospheric pressure and sterilize the inner surface of vials. For this purpose, the RF field was imposed in the bottle by a straight wire and a coil wrapped around the outside of the vial acted as the reference electrode to close the RF circuit [corona-type discharge]. Menashi was able to sterilize vials containing 10^6 spores in times of less than one second. It was found necessary that the plasma contacted the interior surface of the vial and, for this reason, it was thought that the biocidal action was due to intense heating of the spores in a time too short to appreciably heat the glass container, this mechanism was later termed microincineration [Peeples and Anderson, 1985a].

Further patents by Ashman and Menashi [1972] as well as by Boucher (Gut) [1980] and Bithell [1982] showed that an electrical discharge in an appropriate gas (or gases) could lead to sterilization. Boucher (Gut) [1980] also realized sterilization with a microwave-sustained discharge at 2450 MHz (the microwave oven frequency), another ISM authorized frequency. The first systems reported in the scientific literature were of the same nature as those of the patents. More elaborated plasma arrangements were later developed. For example, to sterilize the inner part of vials, a microwave field was applied from the outside and the discharge was initiated by a laser pulse; sterilization times of a few seconds were reported for a 200 W plasma [Tensmeyer et al., 1981].

Most of these early experiments used inert gases, such as argon or helium. However, Ashman and Menashi [1972] added halogens such as chlorine, bromine and iodine within the sterilization chamber to increase the efficacy of the process. Boucher (Gut) [1980] seeded his carrier gas with aldehydes. Instead of rare gases as the carrier gas, Jacobs and Lin [1987] directly used hydrogen peroxide, a sterilant agent, in an aqueous solution in a two-step process: (1) injection and contact of H_2O_2 with the objects to be sterilized; (2) application of an RF discharge ensures that no toxic residues remain on the sterilized items.

3. 2. Discharge Operating Conditions and Identification of Active Species

Discharge operating conditions include the nature, composition, pressure and flow rate of the gas(es) used, the discharge vessel configuration and dimensions, and the applied field frequency. The power absorbed in the plasma is to be considered as a separate parameter [Zakrzewski and Moisan, 1995]; also note that the absorbed power per unit volume (power density), not the absolute value of absorbed power, is meaningful when comparing different experimental arrangements.

Plasma sterilization experiments have been conducted in essentially three pressure domains, which is designated as low pressure (1–10 mTorr range), medium pressure (≈0.1–10 Torr) and atmospheric pressure. In the medium pressure range, there have been experiments under both direct plasma and afterglow exposures.

3. 2. 1. Role of the gas or the gas mixture

Boucher (Gut) [1985] observed that some gases (e.g. CO_2) were more efficient than others [eg argon] to inactivate bacterial spores. He also claimed that spores presoaked for one hour in water are easier to kill. Ratner et al. [1990] showed that plasma sterilization is efficient with most discharge gases (O_2, N_2, air, H_2, halogens, N_2O, H_2O, H_2O_2, CO_2 , SO_2 , SF_6 , aldehydes, organic acids,…), whatever the type of discharge.

3. 2. 2. Power density in the discharge

In his 1980 patent, Boucher mentioned that the power density should be at least 1 mW/cm^3. Boucher (Gut) [1985] further reported that the sterilization efficacy increased with the power density absorbed in the discharge.

3. 2. 3. The role of UV

The possible action of UV irradiation on microorganisms was already raised quite well by Boucher (Gut) [1980] in his extensive patent description: ‘‘The UV high energy photons (3.3 to 6.2 eV) will produce strong cidal effects because they correspond to a maximum of absorption by DNA (deoxyribonucleic acid) and other nucleic acids. However, in the case of spores that can reach one millimeter in diameter, photon energy could be quickly dissipated through the various spore layers and this may restrict photochemical reactions to outer coats. The depth of action of UV photons is restricted to a one micrometer layer. The maximum observed depth for photochemical action in non-oxygen plasmas was 10 μm in the case of polyethylene gelation or ablation. In other words, the photon energy is rather restricted to thin layer surface modifications (changes

in plastics wettability and bondability) and will, therefore, be more efficacious when dealing with the smallest non-sporulated bacteria. In the case of high resistance spores, the photonic action may contribute to partial alteration of the disulphide rich proteins coat and thus facilitate the diffusion of free radicals, atoms, or excited molecules inside the core region'' [Boucher (Gut) 1980]. Boucher's point concerning the limited penetration depth of UV is correct; it is of the order of the spore dimensions, which, as a rule, do not exceed 1–3 μm, but spores can be stacked or aggregated. At any rate, quite surprisingly, Boucher (Gut) [1985] later on concluded that ''the sporicidal action of the plasma is not greatly affected by the presence or absence of UV radiation''.

Tensmeyer et al. [1981], already cited, suggested that the sporicidal action of their plasma was probably due to the radiation it emits since the discharge did not appear to contact the vial walls, but they did not investigate the type and level of photon emission. Peeples and Anderson [1985a] expanded on the work of Tensmeyer et al. [1981] by improving the experimental arrangement of their laser-initiated microwave-sustained discharge (longer plasma duration and reduced power requirement). In a companion paper, Peeples and Anderson [1985b] showed that the laser 'spark' by itself was insufficient for any sporicidal effect, most likely due to its extremely short duration [<5 μs], and therefore inferred that the microwave-sustained discharge was responsible for such an effect. Monitoring the UV emission intensity from their atmospheric-pressure air plasma in the 220–290 nm range, they found that it was about twice the output of a germicidal Hg lamp; from such data, they calculated that their plasma should be able to kill 47 decades of *Bacillus subtilis* within only 0.2 s! Nonetheless, on an experimental

basis, their system could not provide sufficient depyrogenation for serum vials since the level of endotoxin (*Escherichia coli)* destroyed by the plasma was not significant. In fact, photographs taken by them indicated that contact of the vial wall by the plasma was lost one second after plasma ignition. They finally concluded that, even though there was a copious amount of UV radiation emitted by the plasma, the depyrogenation action of the plasma was not the result of the UV light generated by the microwave sustained discharge, but of microincineration.

3. 2. 4. The role of oxygen atoms

Nelson and Berger [1989] showed on *B. subtilis* and *Clostridium sporogenes* that an O_2 plasma could be very efficient as a biocidal medium. Plasma was provided by a reactive-ion etching (RIE) system, where the discharge is achieved between two parallel conducting plates with an RF (13.56 MHz) field. The gas pressure is not specified, most likely in the 0.02–0.2 Torr range. This system accelerates the ions as they drift toward the electrodes on which, presumably, the spores were located. With 200 W, the population of *B. subtilis* was reduced by more than 3.5 $\log_{10}$ in 5 min. *B. subtilis* inactivation with an O_2 plasma had been reported earlier by Fraser et al. [1976], but with a lower efficacy since it required 300 W and 15 min exposure, most probably because of different operating conditions.

3. 2. 5. Influence of the type of microorganisms

To assess the sterilizing efficacy of plasmas, one should test the most resistant microorganisms. Initially, as mentioned by Boucher (Gut) [1985], to legally support a

sterilization claim in the gas phase, the American Environmental Protection Agency (EPA) required tests to be made with two types of aerobic and anaerobic spores (*B. subtilis* and *Clostridium sporogenes*, respectively), while the current standard procedures for checking autoclaves and EtO sterilizers were based on the inactivation of *B. subtilis* and *B. stearothermophilus*. However, Boucher showed that *B. stearothermophilus* was, in fact, a bit more resistant than *B. subtilis* to plasma sterilization (contact with an air plasma at pressures ≈0.6–1.1 Torr), as was later on also reported by Kelly-Wintenberg et al. [1998, atmospheric-pressure air plasma]. In contrast, Hury et al. [1998, low-pressure O_2 plasma] found that *B. stearothermophilus* was easier to inactivate than *B. subtilis*. As for Krebs et al. [1998], they observed that with hydrogen- peroxide plasma-based systems, *B. stearothermophilus* was more resistant than *B. subtilis*. Finally, comparing *B. stearothermophilus* [a spore-forming Gram-positive aerobic rod] and *E. coli* [a Gram-negative facultative rod], Baier et al. [1992], using a medium-pressure plasma [35 MHz discharge in argon within a glass tube], observed that Gram-negative bacteria are more resistant to the process, due to their extra proteins and their lipopolysaccharide walls. Clearly, to be on the safe side, a plasma sterilizer should be initially tested with *B. subtilis*, *B. stearothermophilus* and a Gram-negative bacterium such as *E. coli*.

3. 2. 6. Sterilization of packaged objects

Bithell [1982] showed that sealed packages could be placed in a plasma [O_2 RF-discharge at 40 Pa 0.3 Torr] and the article contained therein sterilized through the package. Sterilizing packaged items raises the question of the active species that can go across the pores of a packaging material: a priori, excited atoms [molecules] and UV

photons should not go through without their concentration and flux, respectively, somehow reduced.

3. 3. First Attempts at Modeling the Inactivation Process

Following the above experiments, a series of interesting hypotheses on the sterilization mechanisms of microorganisms by a gas plasma began to emerge. Nelson and Berger [1989] summarized the situation as follows: ‘‘The specific physiochemical mechanisms responsible for inactivation are not completely understood. Physical sputtering of the outer walls of microbes, chemical degradation by active species in the plasma, and UV light given off by the plasma have all been attributed to the microbiocidal effects of plasma sterilization’’. The first quantitative description of the mechanism of plasma sterilization came from Pelletier [1993]. It is based on erosion, atom by atom, of the microorganism material: gaseous species from the plasma get adsorbed on the microorganism in such a way that volatile compounds are formed, which are pumped out. Such an erosion mechanism of surfaces is known as *etching* in the plasma processing of chips in microelectronics. His model assumes, to a first approximation that the microorganisms are macromolecules mainly made up of carbon, hydrogen, oxygen and nitrogen. Among these elements, carbon is the only one not self-associating to make a volatile molecule, and it must therefore form volatile compounds with other atoms in order to be removed from the surface. In that respect, assuming the chemistry on the surface to occur at thermodynamic equilibrium and considering gas temperatures below 500 K, he showed that in oxygen-based plasmas, from atmospheric

pressure down to pressures as low as 10^{-3} Torr (0.13 Pa), the only (stable) volatile end-product from the combustion of carbon is CO_2, implying that the amount of CO released should be negligible. Then, considering the sequential adsorption and desorption mechanisms of O_2 and O on a surface, he showed that only oxygen atoms can adsorb in the appropriate nearest-neighbor positions in order to efficiently form CO_2 molecules with carbon atoms of the macromolecule. Therefore, this slow combustion of carbon and, as a result, the efficacy of the sterilization process, should increase with the increase of oxygen atoms in the gas phase, until they saturate the surface. Pelletier further showed theoretically that the formation of CO_2 and its subsequent desorption as a volatile compound increases with the temperature of the surface, following an Arrhenius (activation) law: the higher the temperature of the object, the faster should then be the killing of bacteria. Pelletier [1993] did not consider other discharge gases, but conjectured that, in general, the chemically active species from the gaseous phase are radicals (because of their unpaired electrons), excited molecules, and ions. No mention of the role of UV was then made, although it was known that UV photons could take part in the erosion of polymers [for example, Pons et al., 1994; Wertheimer et al., 1999], yielding CO and CO_2 as possible by-products through *photodesorption*, a non-equilibrium chemistry mechanism. The action of ions was discounted on the basis that they would not go across the wrapping paper used to store the sterilized objects.

3. 4. The Case of Plasma-Based Sterilization Systems

In some commercial systems, termed plasma sterilizers, the plasma has no biocidal action, but serves simply as a detoxifying agent, removing noxious residues and limiting the oxidation effect of the highly reactive chemical elements [hydrogen peroxide and peracetic acid-based mixture, respectively] that are injected in the form of vapors as the sterilizing agent [Krebs et al., 1998]. The survival curve of such systems exhibits a unique straight line [Cariou- Travers and Darbord, 2001], as with conventional sterilizers, in contrast to true plasma sterilizers. As a matter of fact, these systems, although efficient, are not plasma sterilizers. The gas or gases used have no biocidal effect unless they are activated by an electrical discharge.

3. 4. 1. Basic principle of plasma-based sterilizers

Living microorganisms are hygroscopic, which means that water vapor in the ambient gaseous phase condenses preferentially on their surfaces. In a similar way, peroxide vapors like hydrogen peroxide and peracetic acid, or oxidative gases like ozone, can condense on nucleation sites such as those formed by bacteria lying on a smooth supporting surface, provided the ambient conditions (pressure and temperature) are appropriate. Viruses, like any surface heterogeneity with dimensions exceeding the critical nucleation diameter (which is approx. 1 nm), are also efficient nucleation sites [Marcos-Martin et al., 1996]. This condensation mechanism is the basic principle of the plasma-based, commercial sterilizers that go through a chemical-gas cycle before the glow discharge is used.

3. 5. Analysis of the Survival Curves and Suggested Mechanisms of Plasma Sterilization

The rate of inactivation of microorganisms exposed to a given stress is most generally exponential and, as such, is adequately reported by their survival curve. We examine such plots for bacterial endospores since they are the most resistant microbial form to environmental stresses including heat, UV radiation and chemicals. Our study is limited to the case of a homogeneous population of spores.

3. 5. 1. Summary of the mechanisms of classical sterilization

Lethal heat energy achieved by wet heat (autoclaves) or dry heat (ovens) leads to the ultimate death of all living forms by destroying the cellular metabolic system, which includes enzymatic components. Wet-heat systems requires a water content sufficient to produce 100% relative humidity at the sterilization temperature, otherwise it is dry heat sterilization.

The high hydrostatic pressure exerted in autoclaves is believed to induce the germination of spores and then to kill the germinated cells. Such a wet-heat process induces several changes in the cell: leakage of low-molecular-weight material through breaches made in the cell wall, RNA and DNA breakdown, and protein coagulation. Inactivation of microorganisms by dry heat may be considered primarily an oxidation process. Figure 3.1 shows a classical survival curve with its unique straight line and three other commonly observed forms, all resulting from thermal inactivation. According to Pflug and Holcomb [1991], curve B corresponds to approximately one-third of the

experimentally determined survival curves for homogeneous cultures of microorganisms exposed to identical [heat] stress conditions. Curves A and D in Figure 3.1 probably constitutes another one-third of the results: during the initial heating time period, the death rate is lower or higher than the major straight-line portion. Curve C is similar to curve A, but tails probably because of a small population of heat-resistant cells. Concave curves similar to curve D are generally interpreted as indicating a heterogeneous population with regard to heat resistance [Moats, 1971]. Chemical sterilization is essentially a process where an item is immersed in the sterilant or exposed to it in a vapor state (chemiclaves, ethylene oxide sterilizers). The corresponding most widely used sterilants are glutaraldehyde, hydrogen peroxide and ethylene oxide.

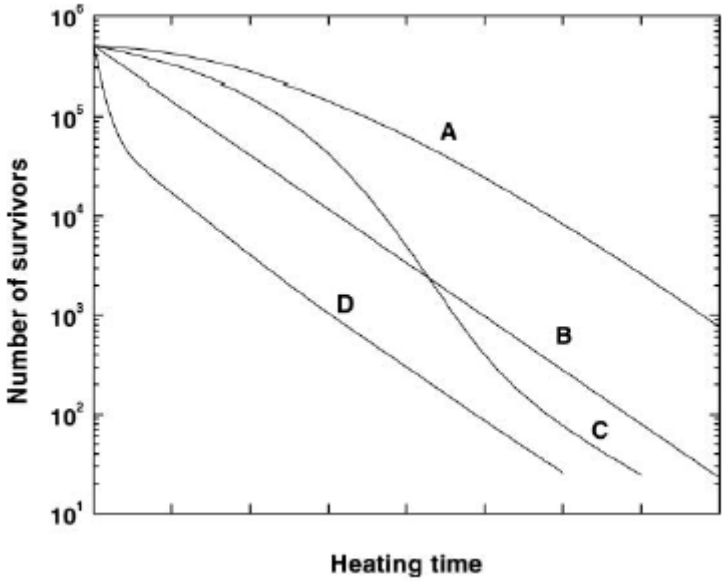

Figure-3.1 Classical survival curve (B) and three other commonly observed non-exponential survival curves. The curves A, C, and D designated as convex, sigmoid and concave curves respectively, resulting from thermal inactivation [Moats, 1971].

The biocidal activity of ethylene oxyde is due to alkylation of different chemical groups in the spore or the vegetative cell. The biocidal effect of glutaraldehyde resides in its interaction with outer cell-layer proteins and glycoproteins, and with the inhibition of RNA, DNA and protein synthesis. Hydrogen peroxide is a strong oxidant and, at high concentrations (10–30%), it is biocidal; the hydroxyl radical produced during its action is believed to do the actual killing of microorganisms by attacking the membrane lipids, DNA and other essential constituents [Morris, 1970]. It generally yields straight-line survival curves such as curve B in Fig. 3.1 [Block, 1991].

3. 5. 2. The active species and the mechanisms involved in plasma sterilization

Plasma sterilization implies completely different mechanisms than those of classical sterilization techniques. Our interpretation of the survival curves assumes the three following basic processes:

1. Direct destruction by *UV irradiation* of the genetic material of the microorganism.

2. Erosion of the microorganism, atom by atom, through *intrinsic photodesorption*. Photon-induced desorption results from UV photons breaking chemical bonds in the microorganism material and leading to the formation of volatile compounds from atoms intrinsic to the microorganism. The volatile by-products of this non-equilibrium chemistry are small molecules (eg CO and CH_x should then be possible).

3. Erosion of the microorganism, atom by atom, through *etching*. Etching results from the adsorption of reactive species from the plasma (glow or afterglow) on the microorganism with which they subsequently undergo chemical reactions to form volatile compounds (spontaneous etching). The reactive species can be atomic and molecular radicals, for example O and OH, respectively, and excited molecules, for example, the 10^2 singlet state. This chemistry, under thermodynamic equilibrium conditions, yields small molecules (eg CO_2, H_2O), which are the final products of the oxidation process. In certain cases, the etching mechanism is enhanced by UV photons [UV induced etching], the photons acting synergistically with the reactive species, thereby accelerating the elimination rate of microorganisms. This UV-induced chemistry under non-equilibrium conditions can result in desorption of radicals and molecules, at both the intermediate and final stages of oxidation. In both cases 2 and 3, the by-products are removed through pumping (or gas flushing) and the gas phase is replenished with 'new' reactive species.

In the pure form of plasma sterilization, the gas or gases involved have no biocidal effect unless they are activated by the electric field of the discharge. The corresponding active species are present only when the discharge is on and disappear some milliseconds after the discharge has been turned off, which means that no vent time is required.

True plasma inactivation (in contrast to plasma-based techniques) is characterized by the existence of two or three distinct phases in the survival curve of a homogeneous population of spores. These phases correspond to changes in the dominating kinetics of the inactivation process as a function of exposure time. In the case of medium and low-pressure discharges, the inactivation mechanisms are the DNA destruction by UV irradiation and the erosion of the microorganism through intrinsic photodesorption and etching (eventually enhanced by UV radiation). These elementary mechanisms clearly set plasma sterilization apart from all other sterilization methods. In that respect, the inactivation of abnormal prions, which have no genetic materials, could a priori be achieved through the erosion of these proteins. In this case, etching enhanced by UV radiation would be the fastest erosion mechanism. The operating conditions would then correspond to those for the shortest sterilization time of microorganisms, but the required time to inactivate prions might be longer because it could necessitate a higher degree of erosion.

The controversy concerning the respective roles of UV photons and reactive radicals has been resolved in the case of reduced-pressure plasma sterilization. A synergistic action of UV photons and O atoms is actually required to minimize the sterilization time; in the case of the N_2–O_2 mixture, the percentage of O_2 should be set such that the UV radiation from the NO_β band is maximized.

The use of UV lamps or lasers in ambient air instead of plasma restricts the erosion of microorganisms to photodesoprtion, a less efficient mechanism than etching. It

also leads to shadowing effects (which includes the difficulty to sterilize crevices), in contrast to gas plasma sterilization where the UV photon is brought to the appropriate site by its emitting atom or molecule. Direct exposure to plasma yields shorter sterilization time than exposure to the plasma afterglow, the latter being generally safer, easier and less expensive to operate. Of the three pressure ranges considered, the low-pressure (mTorr) regime yields the longest sterilization time because of its lowest concentration in neutral active species.

An important shortcoming of plasma sterilization is its dependence on the actual 'thickness' of the microorganisms to be inactivated since the UV photons need to reach their DNA material. It implies that any material covering microorganisms increases the time required to achieve sterilization since erosion, a slow process, has to come into play. In the future, reports on plasma sterilization should specify both the initial number of spores and the surface covered by the suspension, and include some indications as to the organic load or 'cleanliness' of the suspension.

CHAPTER 4

Experimental Setup

The experimental arrangement of the reactor and the two different modes of operation of the atmospheric pressure plasma that was used in the experiments are enumerated. The basic reactor setup consists of top high voltage electrode, grounded electrode and an unglazed ceramic slab as shown in the Figure 4.1. The top high voltage electrode together with the unglazed ceramic material acts as a single resistive electrode. The ceramic material is moistened with water on the side opposite to the discharge. This unique feature of the discharge of resistive electrode composed of unglazed ceramic moistened with water on the side opposite to the discharge prevents a high current discharge from constructing into an arc, and will run for hours at hundreds of watts.

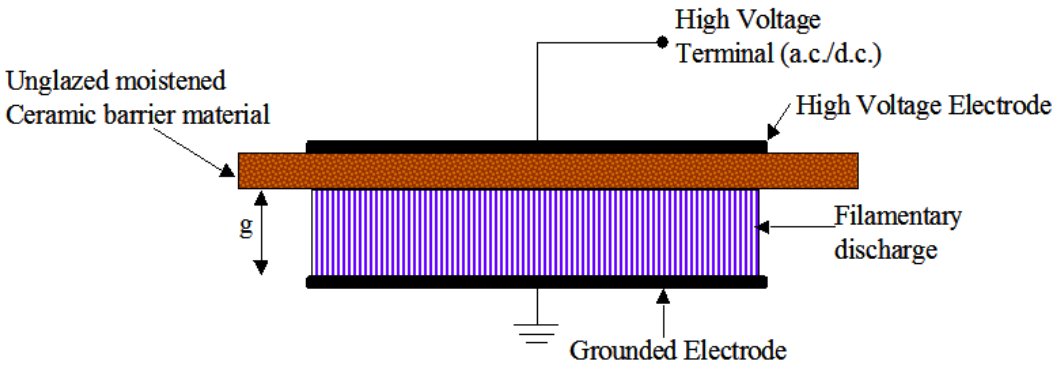

Figure-4.1 Schematic diagram of the resistive barrier discharge setup

The Figure 4.1 represents the discharge operated with air as the ambient gas. By using air as the ambient gas the discharge height or the gap distance between the electrodes (g) is not too large (10 mm and below). It was found that if the noble gases such as Helium or Argon were used as the ambient gas between the electrodes a large volume (in liters) of plasma could be generated. The Figure 4.2 shows the schematic representation of the discharge with a noble gas the working gas. In this setup the gap distance (G) can be too high and it usually requires a closed chamber to keep the ambient gas in the discharge volume. This ability of generating gaseous discharges in large volumes and at atmospheric pressure renders them very practical for various industrial applications. The added advantage of this reactor setup is, it does not require RF power supply.

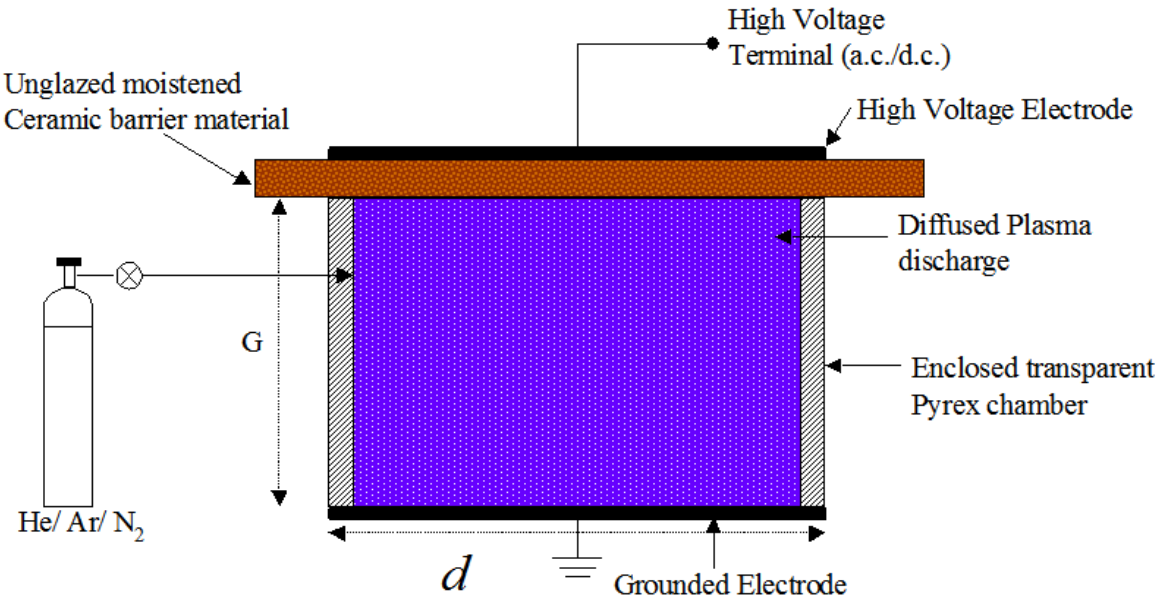

Figure-4.2 Schematic representation of a diffused barrier discharge

Most of these atmospheric pressure gaseous discharges use RF power supplies, which can be expensive and which pose the problem of emitting stray electro magnetic (EM) radiation. This radiation can affect sensitive electronics located in its proximity. To alleviate this drawback we have developed the resistive barrier discharge, which can be operated with direct current (dc) or alternating current (ac) (60 Hz) power supplies as shown in Figure 4.3. This discharge is based on the dielectric barrier (DBD) configuration, but instead of a dielectric, a high-resistivity (few mega ohms/centimeter) sheet is used to cover one or both of the electrodes. This high-resistivity sheet plays the role of distributed resistive ballast, which inhibits the discharge current from reaching a high value, and, therefore, prevents arcing. This ceramic electrode comprises two components; a resistor due to the moisture contained and a capacitor due to the ceramic. Due to the added advantage of the resistive components the discharge can be operated either with dc or ac (60 Hz) power supplies.

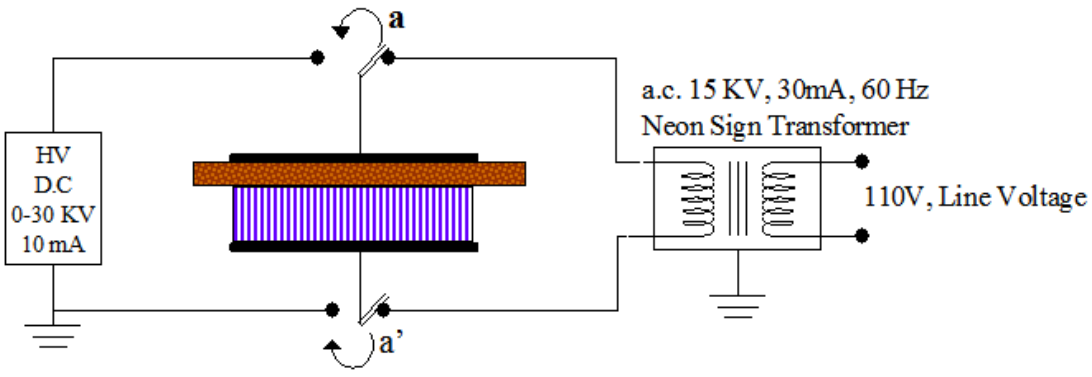

Figure-4. 3 Schematic representation of the power supply unit of the reactor

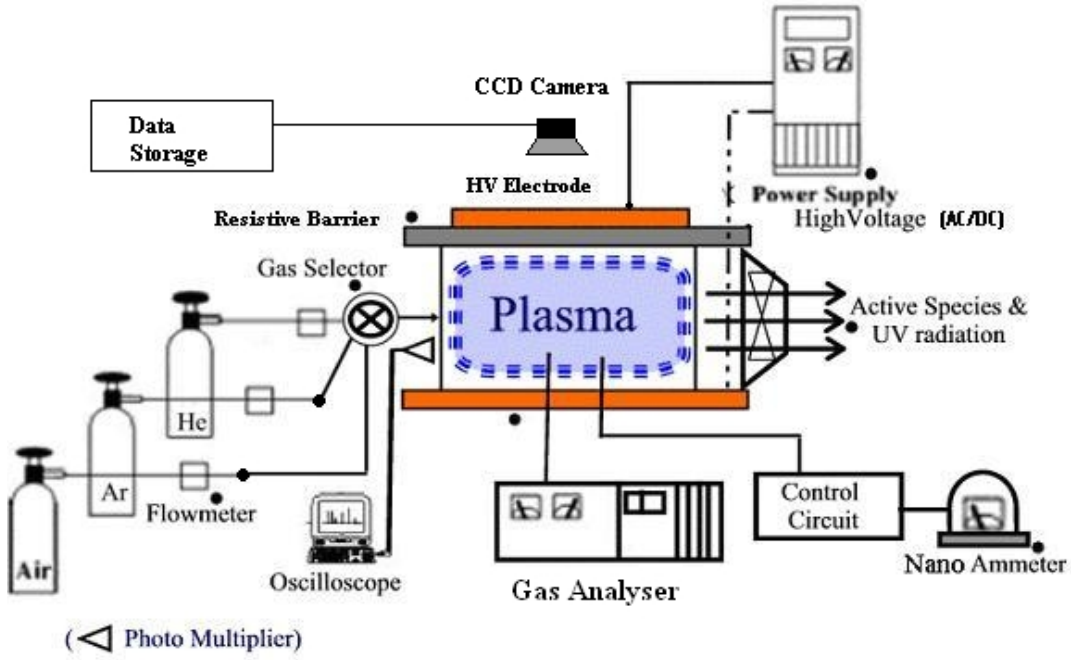

Figure-4.4 Schematic representation of the discharge and diagnostic setup

The general setup of the discharge and its diagnostic setup are shown in Figure 4. 4. The reactor system consists of four subsystems namely reactor sub-system, gas flow sub-system, power supply sub-system, and plasma diagnostics sub-system.

The reactor sub-system consists of two 20 cm x 20 cm, square shaped plane electrodes separated by an insulating support which provides a closed volume for the discharge column. In the discharge column the top electrode is covered with a wetted high resistive unglazed ceramic material of 10 mm thickness and of size 25 cm x 25 cm. The slightly bigger sized resistive layer avoids the direct arc formation between the two electrodes.

In reference with the gas flow sub-system the type of working gas used in the reactor is one of the few key factors for the space between the two electrodes. The experimental results show that the noble gases such as helium and argon can form uniform diffused plasma glow discharge for a large volume at its steady state.

Remarkably if helium or argon is used as a working gas then a uniform glow discharge of plasma is created (shown in Figure 4. 5) for a large volume of 1800Cm^3 with a height of 5 inch (approx). The volume of plasma produced at atmospheric pressure renders them very practical and applicable for various industrial applications, which require large volume of plasma. On the other hand with atmospheric air as the working gas the volume of the plasma produced is significantly less. At room temperature with atmospheric air as the working gas, uniformly distributed filamentary plasma of thickness (height) 1 – 1.5 cm and a volume of 600 Cm^3 was generated and is shown in Figure 4. 6.

The power supply subsystem consists of two power supplies, namely 0-30 KV, DC power supply and 15 KV, 60 Hz AC power supply, an impedance matching network, and a mode selector. In general most atmospheric discharges widely use high frequency RF power supplies to generate plasma of just few millimeters thick. These RF power supplies can be uneconomical and also pose the drawback of emitting stray electro magnetic radiation. These radiation effects may cause damage to electronic devices in its close proximity, which are sensitive to these EM radiations. Our present reactor system will mitigate these draw backs to a great extent.

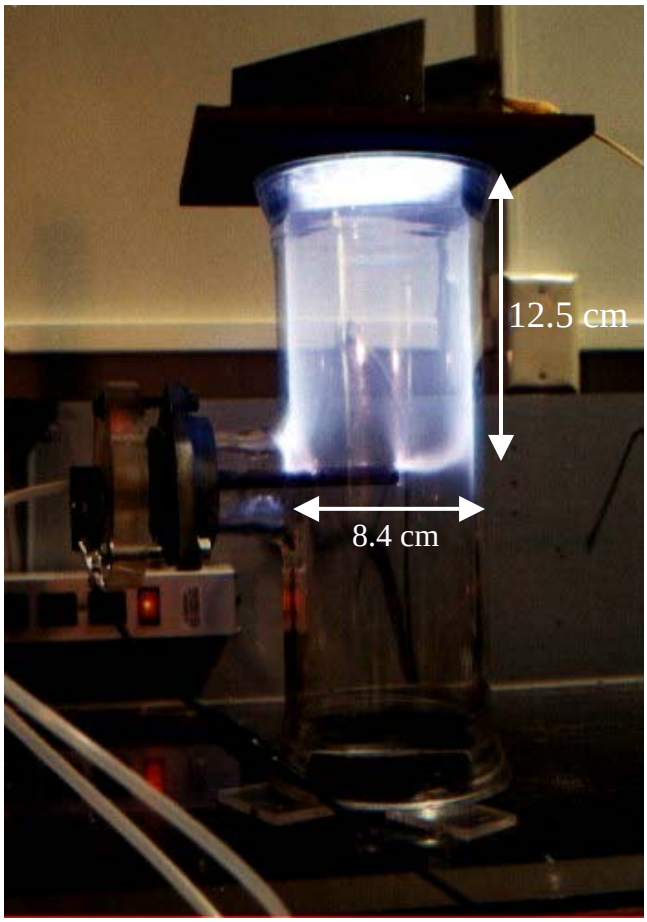

Figure-4.5 Helium discharge

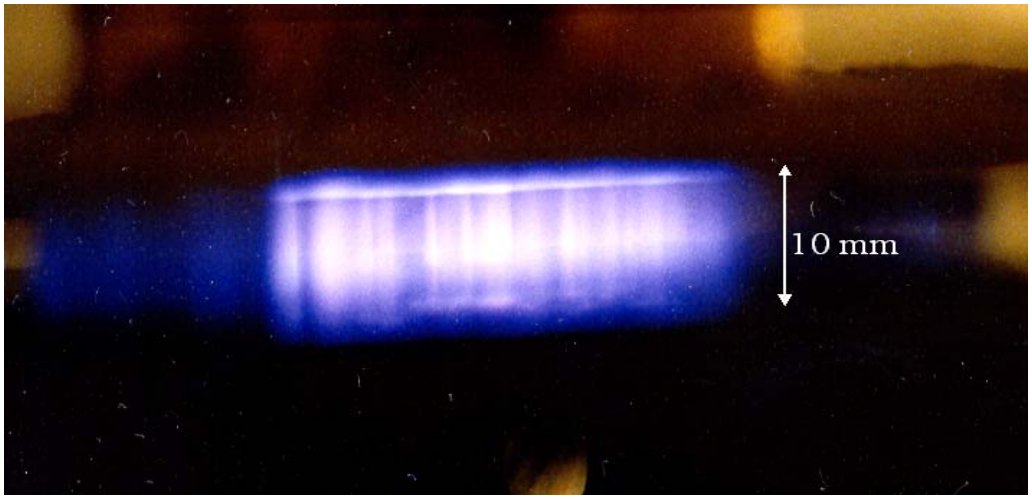

Figure-4.6 Resistive barrier plasma discharge working in atmospheric air

The discharge is capable of operating with either of the two different modes of power supply, such as DC power supply of 30 KV and 10 mA (supply limit) and with low frequency line power supply of 120 V, 60 Hz fed through a neon-sign step-up transformer, which produces an output voltage of 15 KV across its two secondary terminals. These two terminals supply the voltage to the upper and lower electrodes. The power supplies are connected through an appropriate impedance matching network for efficient power coupling. The applied voltage and the gas velocity can characterize the atmospheric pressure DC glow discharge. The voltage induces an electric field in which electrons gain kinetic energy.They collide with gas particles and ionize them if their energy is sufficiently high. With increasing voltage the electrons gain more energy and the number of ionization events grows. This yields an exponential relationship between the discharge current and the voltage. The reactor is provided with a fan, which generates a flow of ambient air with a gas velocity up to 230 cm/sec, as shown in Figure 4. 7. Since the plasma is produced at a steady state between the electrodes through a highly resistive layer, it does not require high velocity gas flow system employed in barrier less atmospheric discharges.

The reactor diagnostics subsystem includes the reactive species measurement using a gas analyzer, gas flow control, a selector to choose the type of gas among Helium, Argon and Atmospheric air. The optical characteristics were measured using a photo multiplier connected to an oscilloscope. The synchronous diagnostics of electrical and optical means of the discharge were analyzed. These methods can detect short pulses.

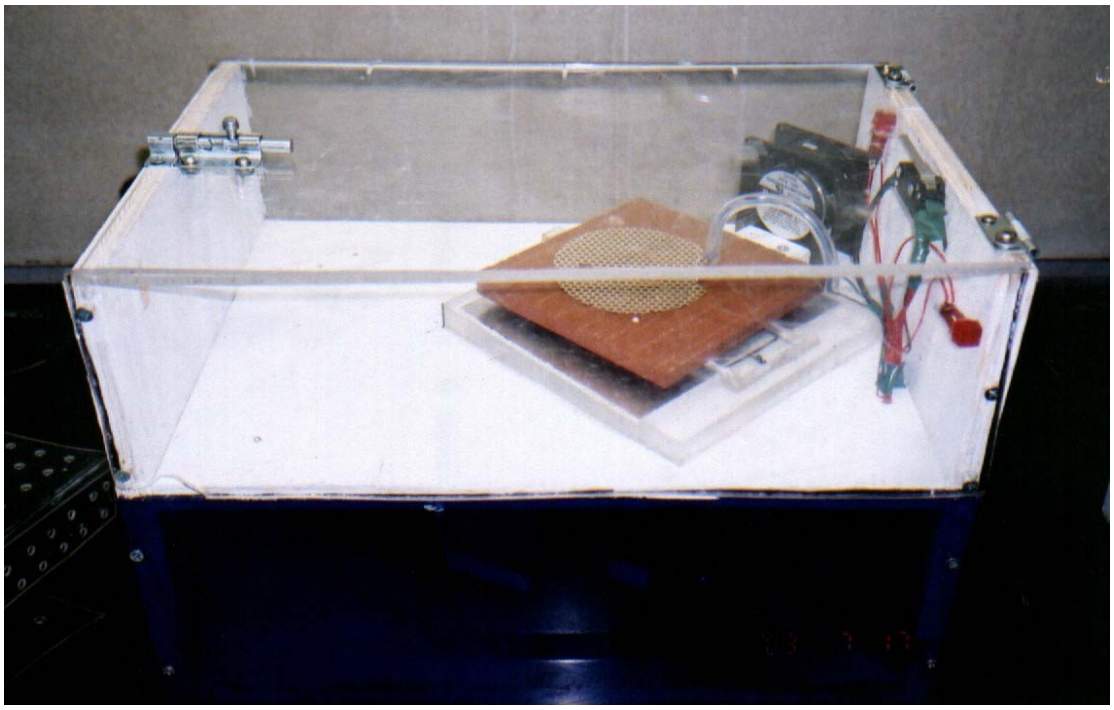

Figure 4. 7. The experimental setup of ionizer

A separate circuit is used to measure the ion population in the discharge chamber. The circuit contains two sets of ion collecting plates placed in a close vicinity to the discharge, in such a way that the ions are collected and which charges the capacitor of 0.027 μF, and energized with a dc voltage source (0-100V battery) connected across the ions collecting plates. The charging rate of the capacitor is proportional to the ion population in the discharge chamber. The charge in the capacitor is measured after different time durations and results are processed**.**

The ion measurements were very successful, using the novel technique. The basic problem was that the ion current detector measured nanoamperes and the electrical noise

from the discharge jammed the detector. We overcame this problem by the above-mentioned method, in which the charge collected was measured after the discharge was turned off. The measurements indicated that an ion density of 10^{12} ions per cubic centimeter was present in the discharge.

The optical investigation was looking for far (chemically active) ultra violet. As a tool we used a crystal of calcite (calcium carbonate) naturally activated with mercury to detect the presence of UV emission. This crystal is phosphorescent for several seconds when activated with far ultraviolet, but ignores (chemically inactive) or visible light. The result is that the far ultraviolet light production was negligible as compared to that of a 150-Watt mercury arc in a quartz tube.

CHAPTER 5

Characteristic Analysis

5. 1. Sheath Structure Analysis in Atmospheric Pressure Barrier Discharge

The knowledge of the electro-dynamic properties of the plasma-sheath boundary is of great importance in number of plasma problems such as electrode phenomena, plasma probes, radio frequency and barrier discharges. The sheath structure analysis depends on the detailed description of the structure requirements [Godyak, 1990]. All electrons are in equilibrium with the electric field, and that the ionization in the sheath can be neglected. Here the sheath structure is analyzed in four different cases of increasing ion energies.

5. 1. 1. Fixed Ions (Transient Plasma Sheath)

The transient sheath can easily be described mathematically [Alexeff, 1969].

$$\frac{d^2V}{dx^2} = -\frac{en_0}{\varepsilon_0} \tag{5.1}$$

V is the applied voltage, x is gap distance, e ion charge, n ion density, ε_o is permittivity of vacuum. Integrating the equation (5.1) twice with respect to the gap distance gives the sheath voltage;

$$\frac{d\ V}{dx} = -\frac{en_0 x}{\varepsilon_0} + C_1$$

$$V = -\frac{en_0 x^2}{2\varepsilon_0} + C_1 x + C_2$$

at sheath edge,

$$E = -\frac{d\ V}{dx} = 0$$

therefore

$$C_1 = \frac{en_0 x_0}{\varepsilon_0}$$

$$V = -\frac{en_0 x^2}{2\varepsilon_0} + \frac{en_0 x_0 x}{\varepsilon_0} + C_2$$

at sheath voltage, V=0, therefore

$$C_2 = -\frac{en_0 x_0^2}{2\varepsilon_0}$$

substituting C_1 and C_2 in the voltage equation we get,

$$V = -\frac{en_0}{\varepsilon_0}\frac{x^2}{2} \tag{5.2}$$

This voltage is also equivalent to the sheath breakdown voltage. Sheath ends at V = 0; and the scaling law is, $V \propto x^2$. The sheath breakdown distance is given by,

$$x = \sqrt{\frac{2\varepsilon_0 V_0}{en_0}} \tag{5.3}$$

Based on the experimental dimensions ($V_o = 10^4$, $n_o = 10^{18}$ per cc) the sheath breakdown distance is approximately equal to 1 mm.

5. 1. 2. Ions have energy that is primarily thermal and less than drift energy

$$v = KE = -K\frac{dV}{dx} \tag{5.4}$$

v is ion drift velocity, K is mobility constant.

$$nv = n_0 v_0 \tag{5.5}$$

n_o is initial ion density, v_o is initial ion velocity. Substituting the ion drift velocity in (5.5) we get,

$$n = \frac{n_0 v_0}{v} = -\frac{n_0 v_0}{K\frac{dV}{dx}} \tag{5.6}$$

Substituting (5.6) in (5.1) we get,

$$\therefore \frac{d^2V}{dx^2}\frac{dV}{dx} = \frac{en_0 v_0}{\varepsilon_0 K}$$

Let $$\frac{dV}{dx} = U; \frac{d^2V}{dx^2} = \frac{dU}{dx}$$

$$\frac{dU}{dx}U = \frac{en_0 v_0}{\varepsilon_0 K}$$

Integrating the above equation we get, $\frac{U^2}{2} = \frac{en_0 v_0 x}{\varepsilon_0 K} + C_1$

$$U = \sqrt{\frac{2en_0 v_0 x}{\varepsilon_0 K} + 2C_1}$$

$$let C_1 = 0, when \frac{dV}{dx} = 0$$

There is no electric field when $\frac{dV}{dx} = -E$, $x = 0$ (end of sheath)

$$\int U = V = -\frac{2}{3}\sqrt{\frac{2en_0v_0}{\varepsilon_0 K}}.x^{\frac{3}{2}} + C_2$$

$$let C_2 = 0, when V = 0$$

There is no potential when x = 0 (end of sheath), simple normalization. Therefore,

$$V = -\frac{2}{3}\sqrt{\frac{2en_0v_0}{\varepsilon_0 K}}.x^{\frac{3}{2}} \qquad (5.7)$$

where x is minus. In this case the end of the sheath is set at zero (x = 0). The start of the sheath is at a negative value for x.

5. 1. 3. Ions have energy that is higher than thermal drift energy

$$v = \frac{eE}{m}t, \quad s = \frac{1}{2}\frac{eE}{m}t^2; \text{ mean free path}$$

$$t = \sqrt{\frac{2sm}{eE}} \text{ and therefore, } v = \sqrt{\frac{2seE}{m}}$$

the above velocity v is $v_{max.}$ The average velocity $\bar{v}$ is one half of $v_{max.}$

$$\bar{v} = \frac{1}{2}\sqrt{\frac{2seE}{m}} \text{ and from equation (5.6), } n = \frac{n_0v_0}{v}$$

Using these sets of values the following relation can be obtained in the same way as case II,

$$V = \left(\frac{3}{5}\right) \times \sqrt[\frac{2}{3}]{3.\frac{en_0v_0}{\varepsilon_0\sqrt{-\frac{2se}{m}}}}.x^{\frac{5}{3}} \qquad (5.8)$$

In this too x = 0 is the sheath edge, and x_0 is a minus number.

5. 1. 4. Free Fall Sheath

$$\frac{d^2V}{dx^2} = -\frac{en}{\varepsilon_0} = -\frac{en_0v_0}{\varepsilon_0\sqrt{-\frac{2eV}{m}}}$$

$$\frac{d^2V}{dx^2}(-V)^{\frac{1}{2}} = -\frac{en_0v_0}{\varepsilon_0\sqrt{\frac{2e}{m}}} = -C_0 \tag{5.9}$$

To simplify the calculation, let us assign,

$$V = ax^j \tag{5.10}$$

$$\frac{dV}{dx} = ajx^{j-1}$$

$$\frac{d^2V}{dx^2} = aj(j-1)x^{j-2}$$

Substituting back to the equation (5.9),

$$\left[aj(j-1)x^{j-2}\right]\left[-ax^j\right]^{\frac{1}{2}} = -C_0 \tag{5.11}$$

$$j - 2 + \frac{j}{2} = 0$$

$$j = \frac{4}{3}$$

Substituting back to equation (5.11),

$$a = \left[\frac{9}{4}C_0\right]^{\frac{2}{3}}$$

Finally the equation (10),

$$V = \left[\frac{9}{4}C_0\right]^{\frac{2}{3}} x^{\frac{4}{3}}$$

$$V = \left[\frac{9}{4} \frac{e n_0 v_0}{\varepsilon_0 \sqrt{\frac{2e}{m}}} \right]^{\frac{2}{3}} x^{\frac{4}{3}} \qquad (5.12)$$

The theoretical values of the sheath size in the four different cases are shown in the Table 1 for an applied voltage of 10 K volts. The scaling law of the sheath distance with respect to the applied voltage is shown in the Table 2.

Table-1 Theoretical value of the sheath size in four different cases of sheath structure.

Case:	**Sheath**	**Sheath Size (cm)**
I.	Fixed ions	0.10
II.	Ions in gas – low energy	0.15
III.	Ions in gas – high energy	0.52
IV.	Free ions	1.33

Table-2 Scaling law with respect to sheath size in different cases.

Case:	Sheaths	Scaling law	Power
I.	Fixed ions	$V \propto x^2$	2
II.	Ions in gas – low energy	$V \propto x^{\frac{3}{2}}$	1.5
III.	Ions in gas – high energy	$V \propto x^{\frac{5}{3}}$	1.67
IV.	Free ions	$V \propto x^{\frac{4}{3}}$	1.33

5. 2. Free Electron and Ion Population Measurements

The plasma density in the large volume atmospheric helium discharge has been measured by microwave absorption techniques. At atmospheric pressure, the electron – gas atom collision rate is so high that no microwave phase shift can be observed at a frequency of 2.5 GHz. However, an attenuation of the microwave signal is easily observed. Since the plasma is self – pulsing, these pulses create short bursts of electrons that produce an increase in microwave attenuation. The attenuation is small, about one percent, but is clearly visible. The transient free electron density is found to be about 10^{11} per cc. As a secondary benefit, the duration of the attenuation reveals the lifetime of the free electrons before they form negative ions. This is short, on the order of 100 microseconds.

We have used a novel method of finding the ion population in the helium plasma discharge as shown in Figure 5.1. The ion measurements were done successfully, as we used a unique technique. The fundamental problem was that the ion current detector measured nanoamperes and the electrical noise from the discharge jammed the detector. The problem was eliminated by collecting the ion current over an interval in time in a capacitor, and measured the collected charge with a nanometer after the discharge was turned off. Based on this measurement it is found that the discharge has an ion density of 10^{12} ions/cm^3. In the case of filamentary air plasma the electron density can be estimated with pulsing current values. Based on the physical dimensions of the discharge the total charge collected per pulse is found to be 0.4 x 10^{-6} coulomb.

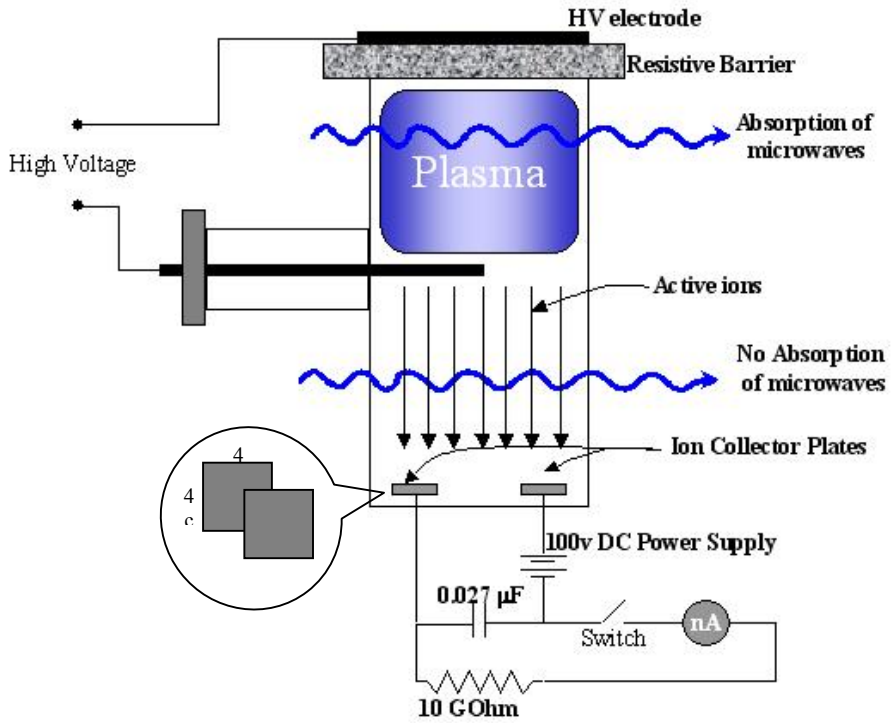

Figure. 5. 1. Ion current measurement technique

If the discharge time is observed to be 1μsec, the current will be 0.4 A (i = Q/t), which is observed both time verse and current verse. The electron density may be estimated from this current pulse.

$$i = (area)en_e v_d \qquad \text{(amps)} \tag{5.13}$$

The electrode area is measured to be 2.25×10^{-2} m^2, v_d is 5 x 10^4 m/sec, using the above values the free electron density is found as 2.8 x 10^8 per cc (10^9 approx.). This does not consider the number of negative and positive ions in the discharge. We have observed by microwave techniques that the free electrons vanish very rapidly. The microwave measurements yield a free electron density of 10^{11} cm^{-3}. The above yield of 10^9 cm^{-3} is based on electron collected. By estimating the ion recombination rate, we can estimate the ion density (N_i) as,

$$ion\,density \quad (N_i) = \frac{N_e \tau_i}{\tau_e} \tag{5.14}$$

N_e is the number of electrons produced per pulse, τ_i and τ_e are ion decay time and pulse repetition time. The ion number density of the filamentary atmospheric air plasma is estimated as follows,

$$1.7 \times 10^{-6} n_i^{\,2} = \frac{dn}{dt} \tag{5.15}$$

The number of collisions per cubic centimeter per second made by 2n molecules per cubic centimeter of air at normal temperature and pressure is of the order of 1.6 x 10^{-10} n^2, whereas the number of recombination per cubic centimeter per second is of the order of 1.7 x 10^{-6} n^2 [17]. Therefore,

$$\frac{dn}{dt} = \frac{Pulse\,magnitude}{time\,between\,pulses} = \frac{10^{11}}{10^{-6}} = 10^{17} \tag{5.16}$$

Substituting (11) in (10) we get the ion density $n_i \approx 10^{12}$ cm^{-3}

5. 3. Ion Diffusion Density as Measured by Ion Diffusion Flux.

We consider the ion diffusion velocity to be a series of random steps. The length of one step, l is the mean free path, the reciprocal of the gas density, n times the scattering cross section, σ.

For one step,

$$l = \frac{1}{n_g \sigma} \tag{5.17}$$

The time for one step is the mean free path divided by the thermal velocity,

$$t = \frac{l}{v} = \frac{1}{n_g \sigma \sqrt{\frac{KT}{m}}} \tag{5.18}$$

Here K is boltzmann's constant, T is the thermal energy of the ions, and the gas atoms, and m is the ion mass. For n steps

$$L = \sqrt{\sum_n l^2} = \sqrt{n} l$$

$$\therefore \frac{L}{l} = \sqrt{n}$$

$$T = \sum t = nt$$

$$v_{driff} = \frac{L}{T} = \frac{l}{t\sqrt{n}}$$

So the velocity is given by

$$v = \frac{L}{T} = \frac{1}{\sqrt{n}} \frac{l}{t} = \frac{l^2}{Lt}$$

Note: the l is one-dimensional element in one-dimensional case. In three dimensional case, with the assumption

$$l^2 = lx^2 + ly^2 + lz^2$$

$$If: l_x = l_y = l_z$$

$$l^2 = 3l_x^2$$

$$l_x = l\frac{1}{\sqrt{3}}$$

The velocity is derived to be, $v = \frac{L}{T} = \frac{1}{3}\frac{l^2}{Lt}$

The gas molecule density is $n_g = \frac{6.02 \times 10^{23}}{22.4 \times 10^3} = 2.69 \times 10^{19}$ gas molecules/cm^3

The mean free path l is $l = \frac{1}{n_g \sigma} = \frac{1}{2.69^{19} \times 10^{-15}} = \frac{1}{3} \times 10^{-4} cm$

Substituting these values in equation (13) we get,

$$t = \frac{l}{\sqrt{\frac{KT}{m}}} = \frac{1}{3} \times 10^{-9} \text{ sec}$$

Substituting the above values in equation (14) for L = 10 cm the velocity ions is found to be 1/9 cm/sec. Based on our data taken from the ion population measurement technique the flux of active ions is found to be 8.58x10^9 ions/cm^2 sec

$$v_0 n_0 = flux$$

$$n_0 = \frac{flux}{v_0} \approx 10^{11} ions/cm^3$$

It is observed that the effect of recombination makes the value of n_0 higher.

5. 4. Pulsing Mechanism and Time Constant

The pulsing mechanism is only observed in the system containing the ceramic electrodes. The Figure 5.2 shows the pulsing discharge current. The yellow traces are current pulses observed by a current pickup on the power feed wire. The blue traces are light signals as observed by a photomultiplier. Therefore the electrodes are considered as a source of the pulses. The proposed mechanism of the self – pulsing of the plasma is a RC oscillator, comprising the ceramic electrode. This electrode contains both a capacitor, due to the ceramic, and a resistor, due to the enclosed water. For one experiment the value of the capacitor was estimated as follows.

Figure 5. 2 Traces of pulsing discharge current

Consider a ceramic slab 6” by 6” by ¼” thick with a relative dielectric constant of 2. The corresponding capacitance is 32.5 x10^{-12} F. The resistance is computed from the applied voltage, 15 KV, and the resulting current, 10 mA. The resulting resistance is 1.5 M ohms. From this, the RC relaxation time is computed to be about 50 microseconds, which is approximately equal to the observed value. Besides, by changing the applied voltage, this time can be modified, as one can go from a part of an RC charging time to several e – fold times. The mechanism is that a plasma discharge charges the capacitor, resulting in no voltage applied to the discharge tube. The charge leaks away, resulting in a rising voltage applied to the discharge tube. The discharge tube ignites, recharging the capacitor, and the cycle repeats. However, the localized glow over the electrodes suggests that a sheath effect also contributes to the mechanism.

The capacitance,

$$C = 2\varepsilon_o \frac{area}{thickness} = \frac{2 \times 8.854 \times 10^{-12} \times 6 \times 6 \times 2.54 \times 10^{-2}}{0.5} \approx 32 \times 10^{-12}\ F$$

The resultant time constant $\tau = RC = (1.5 \times 10^{6}) \times (32 \times 10^{-12}) \approx 50\ \mu sec.$

CHAPTER 6

Chemical Analysis

The chemistry of plasma: “The influence of physical forces, of modes of aggregation and of mass, not only on the result, but on the manner of the transformation of one kind of matter into another kind – in brief, The conditions of chemical change – present a problem to the chemist which only of late years has been submitted to experimental investigation. The difficulties besetting this line of inquiry are many, but the greatest of them is the difficulty of finding a reaction that is simple in kind, that takes place between bodies which can be prepared in great purity, and that yields products, which can be exactly measured” [Dixon 1884]. According to the literature, a great deal of research on the removal of VOCs and NO_x using nonthermal plasma has been carried out so far [Rosocha 1993, Roush 1996, Tas 1997].

The test chamber used for the chemical analysis and ion measurement is shown in the Figure 6.1. Our chemical analysis is based on the reactive chemical gases and components produced by the steady state atmospheric pressure resistive barrier plasma discharge. It comprises of tests of Ozone (O_3), Nitrogen monoxide (NO), Nitrogen dioxide (NO_2), and Methane (CH_4). The chemical analysis was used to carry out by a gas analyzer OMNI 4000 product of ENMET Corporation as shown in Figure 6.2. The OMNI-4000 is a portable multi-gas detector. It can simultaneously detect the presence of up to four gases by means of special sensors.

Figure-6.1 Test chamber prepared for chemical analysis

Figure-6.2 Gas analyzer-OMNI 4000

Thus, depending on the number and type of sensors installed, the OMNI-4000 detects the presence of corresponding gases in the immediate environment. Sensors can be easily removed and replaced by other available sensors for different gases. The sensors of the gas analyzer were calibrated for our experimental requirements, shown in Figure 6.3. The chemical analysis was performed separately for atmospheric air and helium background gases. The results show that the overwhelming production of ozone in both cases of He and O_2 environment. The results were obtained by running the discharge for 60 seconds. From the Figure 6.4 it can be easily observed that the rate of rise of ozone content during discharge run time is very high. With the duration of 60 seconds the ozone content increased to 1.7 ppm maximum. At this time the discharge was turned off. The readings of ozone concentration were recorded continuously till it reaches the insignificant value.

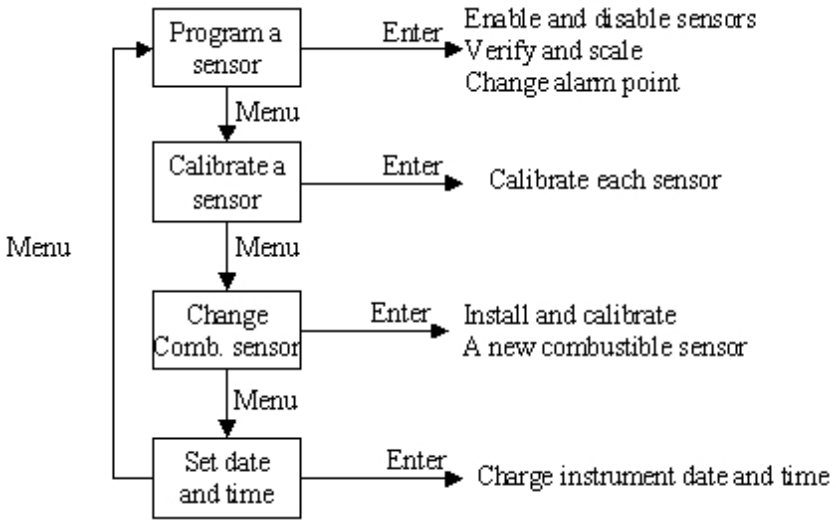

Figure-6.3 The block diagram of the calibration process of the gas analyzer OMNI-4000 for the chemical analysis.

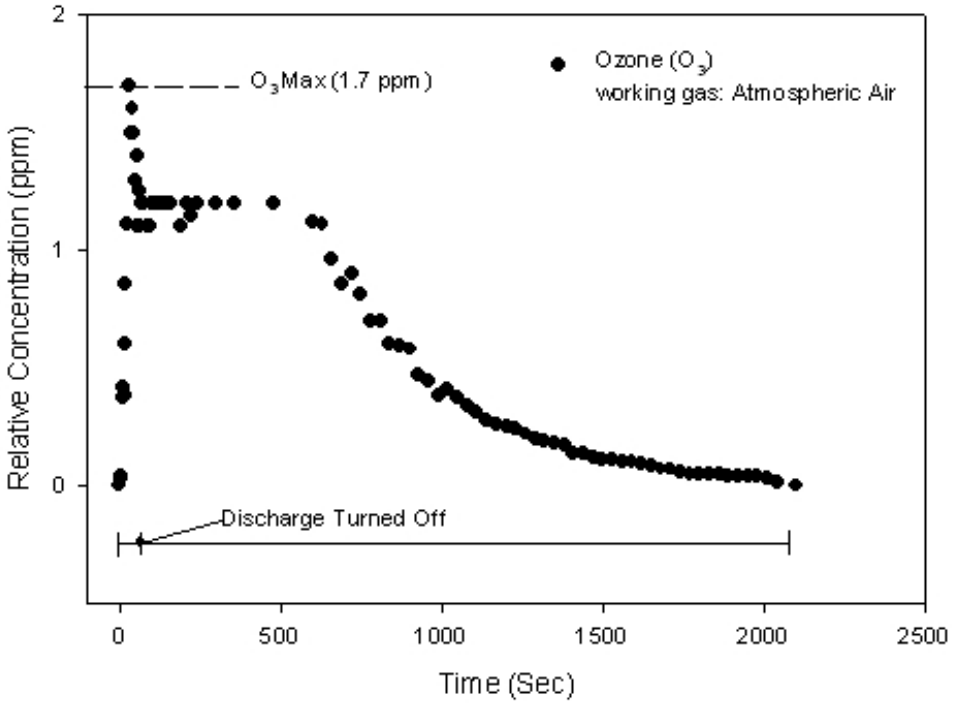

Figure-6.4 Relative concentration of ozone in parts per million (ppm) with atmospheric air background gas. The discharge run time is 60 seconds.

The Ozone persisted for a long time compared to the discharge run time. It is widely accepted that the ozone is one of the prime element of biological decontamination and this reactor produces voluminous ozone in a very short period of time. The OMNI-4000 is used to measure Nitrogen-dioxide (NO_2). The Figure 6.5 shows the NO_2 production and decay rate during discharge on and off time respectively. The NO_2 production rate is far high compared to its depletion rate. Similarly the discharge ran for 60 seconds and the readings were recorded continuously until the NO_2 content reaches the insignificant value. It is found that the overwhelming production of ozone actuated the NO_2 sensor and therefore the NO_2 may not be precise.

The Fig. 6.6 shows the comparison of O_3 and NO_2 concentration in the atmospheric pressure plasma with atmospheric air background on the same scale. The O_3 and NO_2 lasted for a long time. We have also tried to run the discharge for a more than 60 seconds. But due to the overwhelming production rate of the ozone and very high production rate of NO_2 causes the sensor to saturate and causes to alarm the device. The ozone concentration curves of helium and atmospheric air are almost overlapping each other. The Figure 6.7 shows the concentration of O_3 with He background gas. The discharge was turned off at 30 seconds from the start at this point the ozone level was reached 1.6 ppm with a production rate of 0.0533 ppm/sec. The Figure 6.8 shows both the data observed with He and O_2 working gases almost overlaps each other. The discharge ran for 60 seconds and the production rate in both the cases are almost the same. Note that the wet electrode introduces H_2O into the helium, which may be also being a source of the O_3.

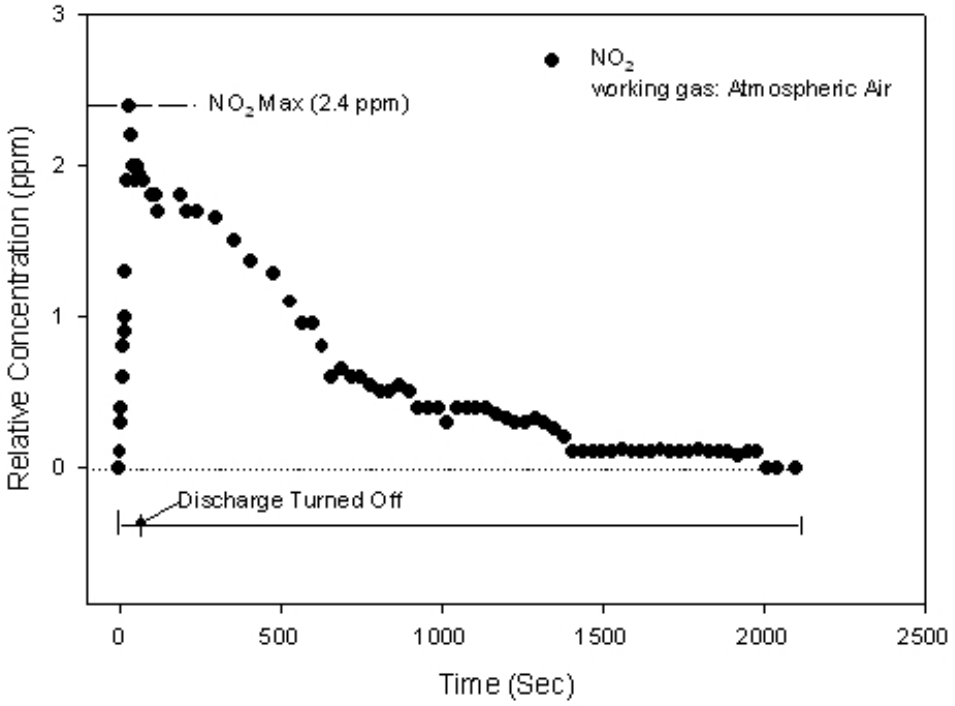

Figure-6.5 Relative concentration of NO_2 in ppm with atmospheric air background gas. The discharge run time is 60 seconds.

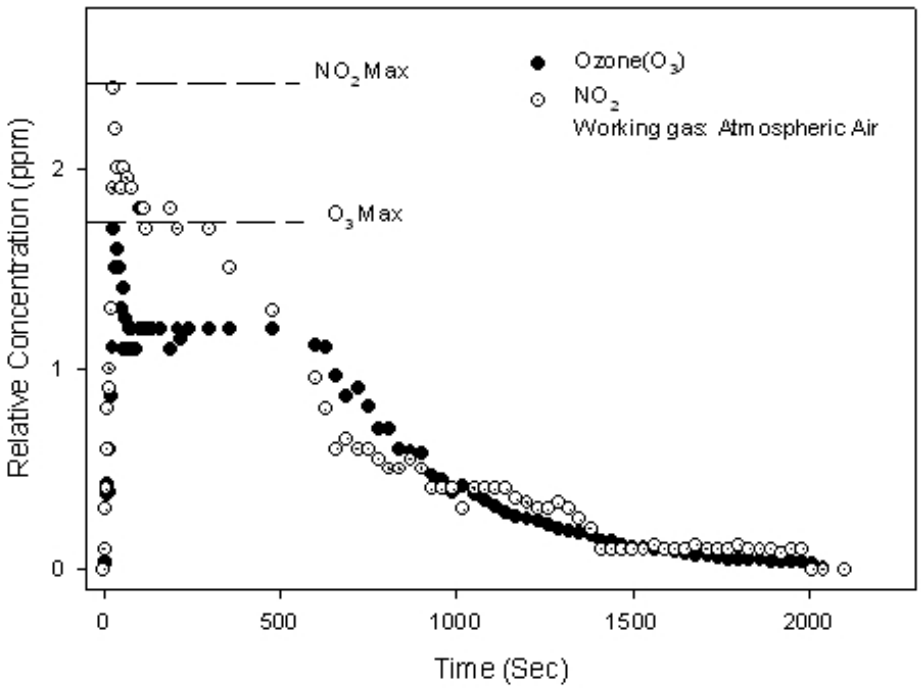

Figure-6.6 Comparison of the relative concentration of O3 and NO2 with atmospheric air background gas. The discharge run time is 60 seconds.

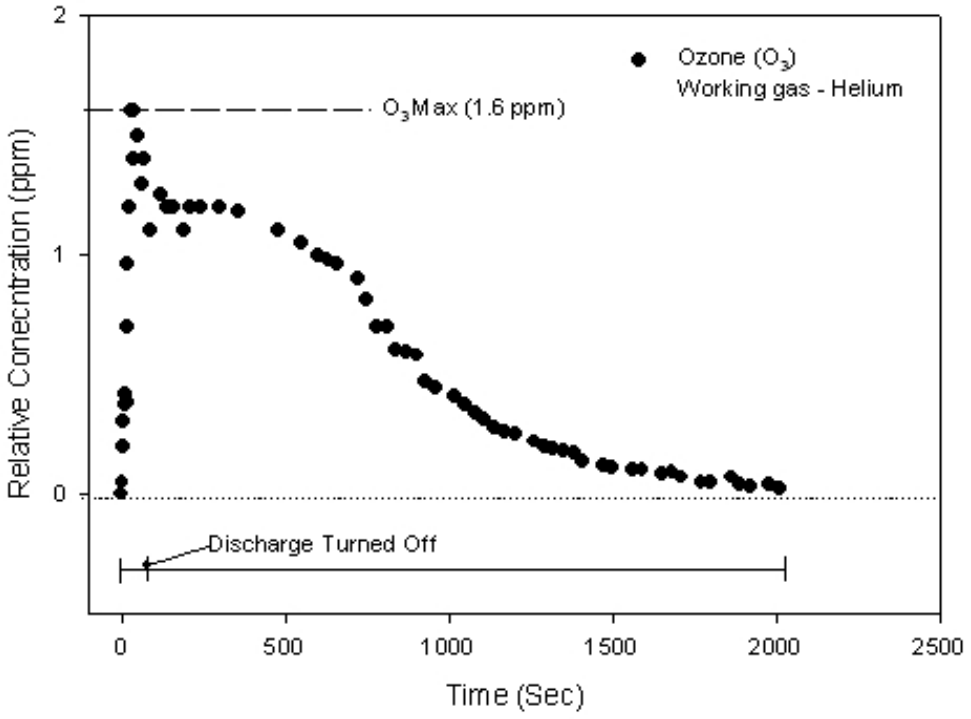

Figure-6.7 Relative concentration of O_3 in ppm with He background gas. The discharge run time is 60 seconds.

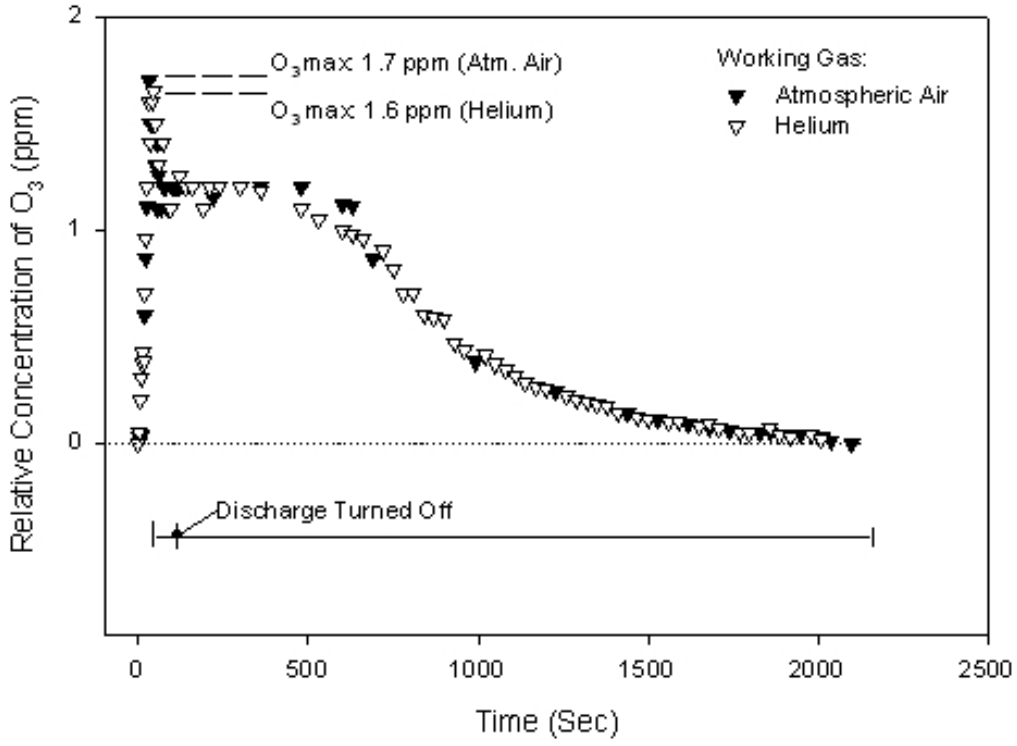

Figure-6.8 Comparison of relative concentration of ozone production with helium and atmospheric air background gases. The discharge run time is 60 seconds.

CHAPTER 7

Optical Analysis

7. 1. Ultra Violet (UV) Measurements

One presumed important germicidal mechanism in barrier discharges is the UV radiation [Moisan 2001]. The continual wave UV light has been used as disinfection tools for nearly a century. More recent investigations, employing these methods simultaneously, have resulted in significant improvements in the inactivation of vegetative and spore forming bacteria. Bayliss and Waites [Bayliss 1982] showed a dependence of the efficacy on the concentration of hydrogen peroxide, and Hartman [Hartman 1979] showed that the process is dependent on the spectral content of the UV. The optical studies have been carried out with the intent of identifying the Ultra Violet (UV) rays from the glow discharge chamber. We have used a new method of identifying the presence of UV rays produced by the plasma. As a tool of detecting UV light we used a calcite crystal (calcium carbonate) naturally activated with mercury as shown in Figure 7.1. This crystal is phosphorescent for several seconds when activated with far ultraviolet**.** It ignores near ultraviolet (chemically inactive) or visible light. The result is that the far ultraviolet light production was negligible as compared to that of a 150-Watt mercury arc in a quartz tube.

Figure-7.1 Calcite crystal activated by mercury

7. 2. Intensity Distribution

The intensity distribution of the glow discharge has been studied to analyze the plasma uniformity across the reactor chamber. The intensity distribution curve from the Figures 7.2 and 7.3 illustrates the distribution of the micro discharges and the plasma uniformity across the plasma chamber. The Figures 7.2 and 7.3 shows plasma discharge generated at atmospheric pressure with atmospheric air as the working gas. It can be observed that the discharge was created for a thickness of 10 mm at atmospheric air and it produces a plasma discharge of reasonable uniformity. The plasma uniformity also depends with the area of electrodes besides the gap distance. In the Figure 7.2 the electrode area is 105 mm x 105 mm with a gap of 10 mm between the electrodes.

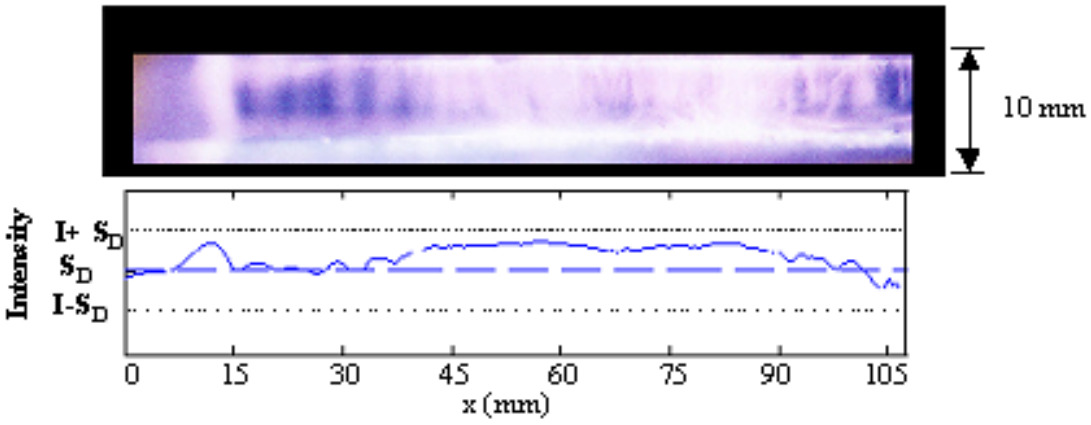

Figure-7.2 Intensity distribution of the filamentary discharge with electrode diameter of 105 mm

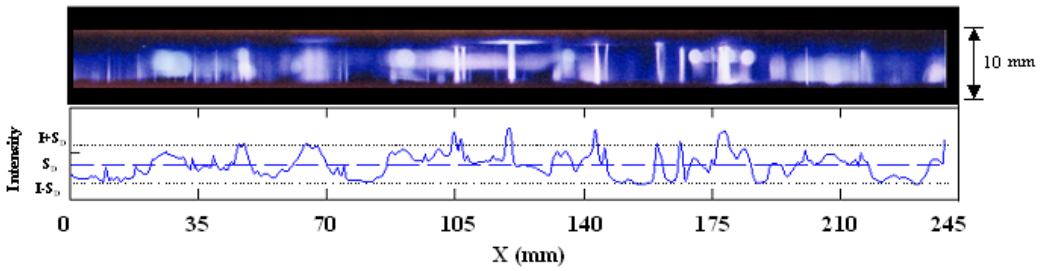

Figure-7.3 Intensity distribution of the filamentary discharge with electrode diameter of 245mm

The important indirect mechanism is observed to be the discharge homogeneity, which is the homogeneity of filamentary micro discharge distribution. In the Figure 7.3 the electrode area was very large, 245 mm x 245 mm. Due to the large electrode area the distribution of micro discharges is non-uniform. Besides, the discharge is capable of running for long discharge time with out arc formation.

7. 3. Transparent Electrode

In general the atmospheric pressure plasma discharge is monitored or visualized across the electrode. It is difficult to identify the distribution and the density of glow discharge in the case of filamentary discharge mode by visualizing it across the electrodes. In order to resolve this difficulty a special electrode is constructed, which is electrically conductive and optically transparent. This transparent electrode is made up of low resistance, vacuum deposited coating of Indium Tin Oxide (ITO). The discharged is operated with transparent electrodes of 60, 100, and 250 ohms per square. The light transmission efficiency of such ITO electrode is very high in general. The ITO used in our experiments has a light transmission efficiency of >86%. In order to capture the top view of the filamentary discharge the reactor system is modified. The bottom ground electrode is chosen as the resistive electrode and the top electrode is Indium Tin Oxide coated glass substrate electrode. The Figure 7.4 shows the schematic representation of the transparent electrode setup.

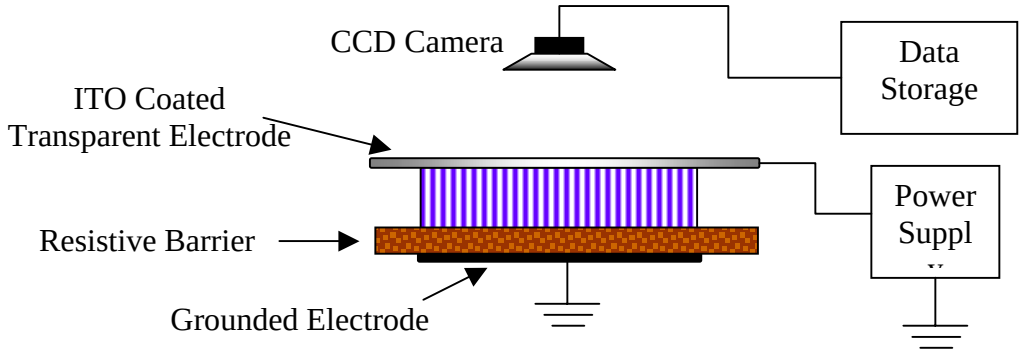

Figure-7.4 Schematic representation of the transparent electrode arrangement

A series of photographs taken with the transparent electrodes are shown in the Figures below. The figure 7.5, 7.6, 7.7, 7.8 shows the distribution of the filamentary discharge using an Indium Tin Oxide (ITO) coated electrode. It is observed from figures 7.7 and 7.8, that the moisture content in the ceramic layer is essential to produce the discharge over a large area. The ITO coated thin film works well as optically transparent and electrically conducting material. The top electrode of the discharge is made of ITO coated substrate for this measurement.

The ITO coated electrode is also tried with the Helium discharge. The Figures 7.9 and 7.10 shows the plan and elevation of the cone shaped discharge with Helium background. In this arrangement the top electrode is grounded and acts as a cathode and the bottom ceramic electrode acts as anode. Besides the transparent electrode the discharge is also tested with a mesh electrode. The mesh electrode works moderately well with the atmospheric discharge. The Photographic images are shown in Figures 7.11 and 7.12.

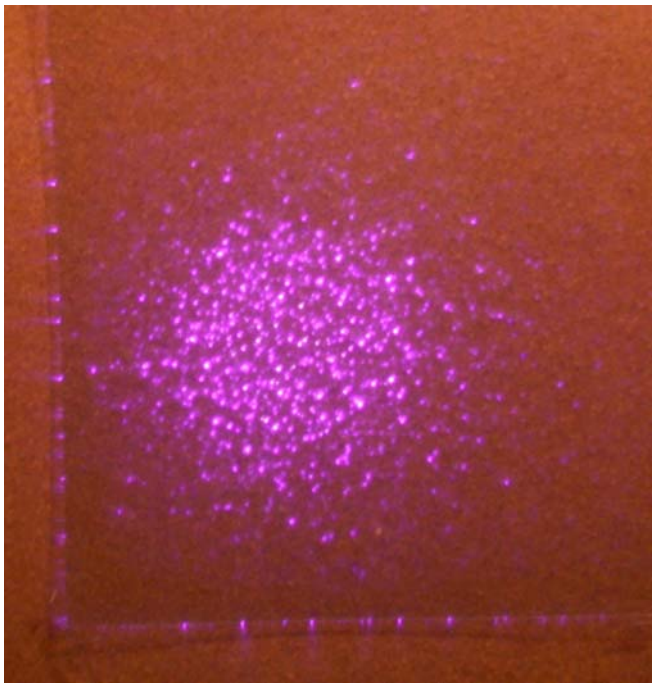

Figure-7.5 Top view of the filamentary discharge - laboratory lights turned on

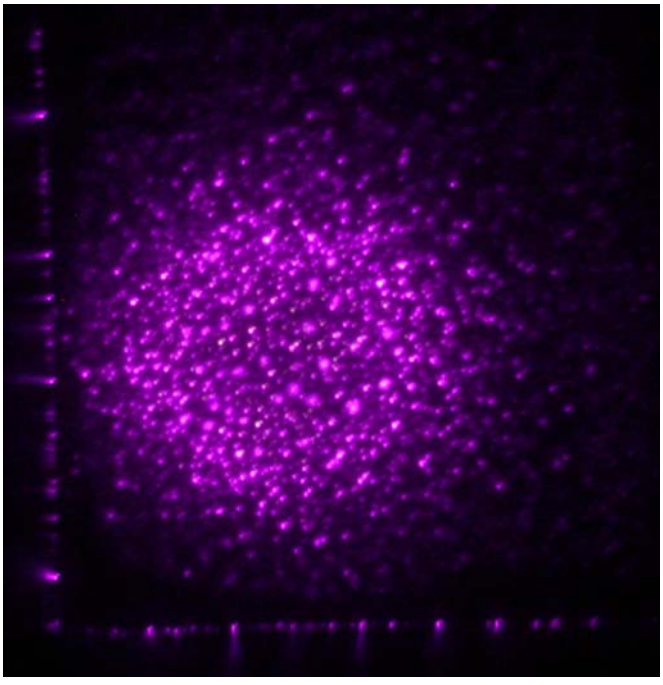

Figure-7.6 Top view of the filamentary discharge - laboratory lights turned off

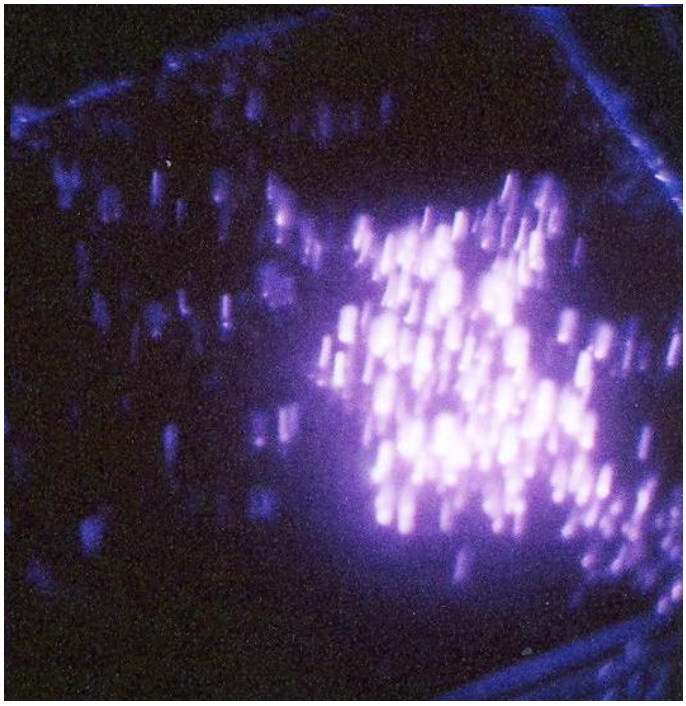

Figure-7.7 Top view of the filamentary discharge with dryer ceramic barrier

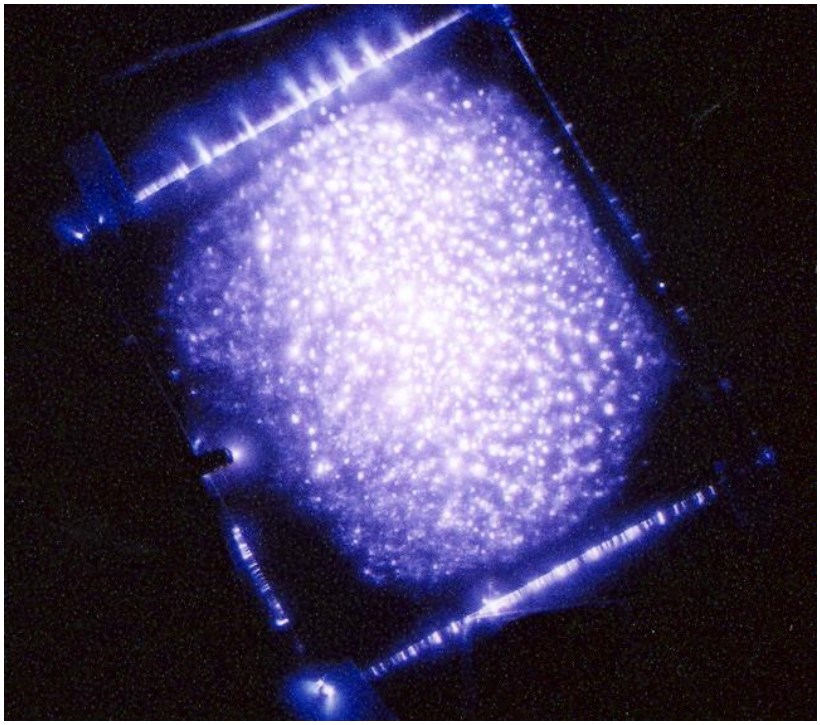

Figure-7.8 Top view of the filamentary discharge with wetter ceramic barrier

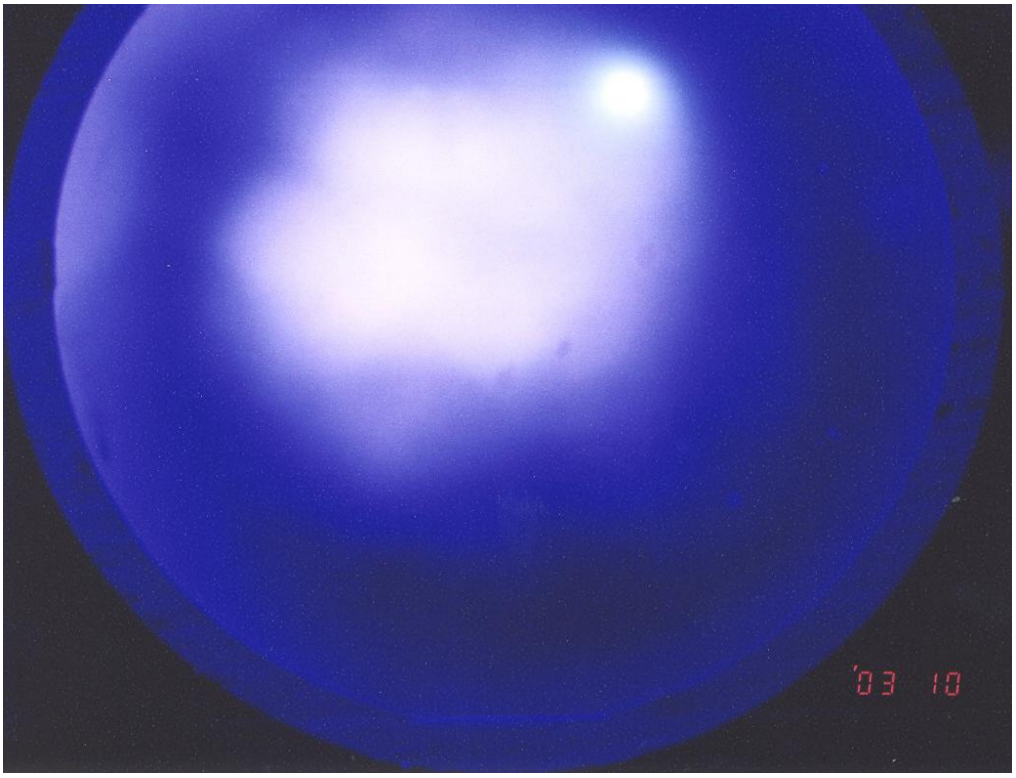

Figure-7.9 Plan of the Helium discharge with ITO coated transparent electrode on the top

Figure-7.10 Elevation of the Helium discharge with ITO coated transparent electrode on the top

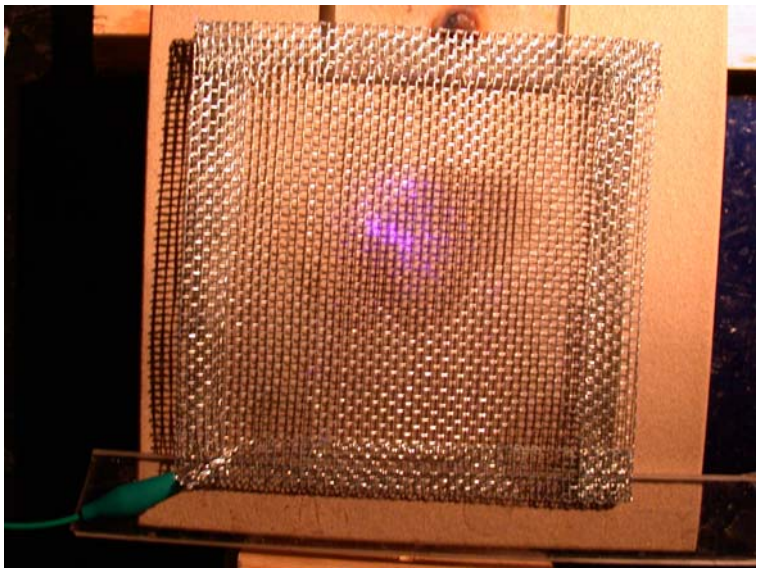

Figure 7.11 Mesh electrode with laboratory lights turned on

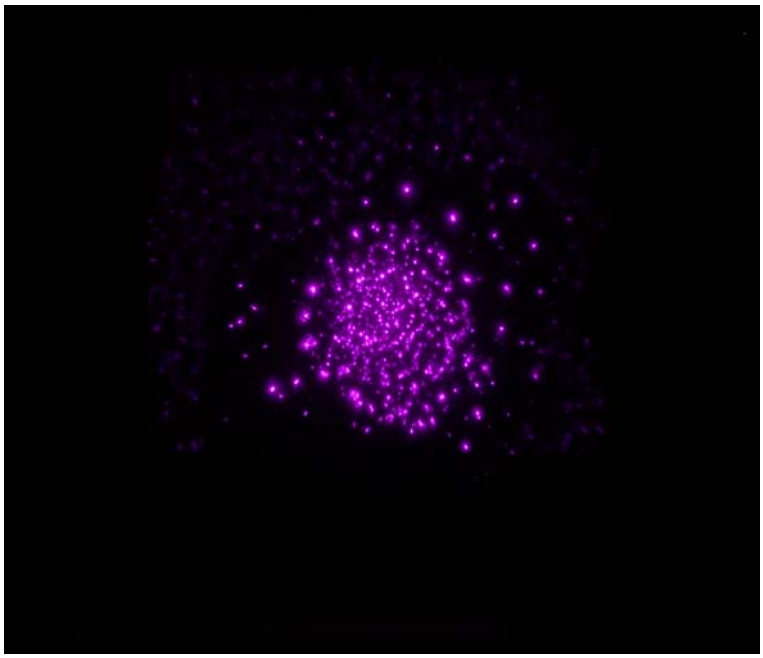

Figure 7. 12 Mesh electrode with laboratory lights turned off

Figure 7. 13 show the helium discharge photographed by a fish eye camera. In this figure both the top and bottom electrodes are viewable simultaneously. Here, both the top and bottom electrodes are ceramic.

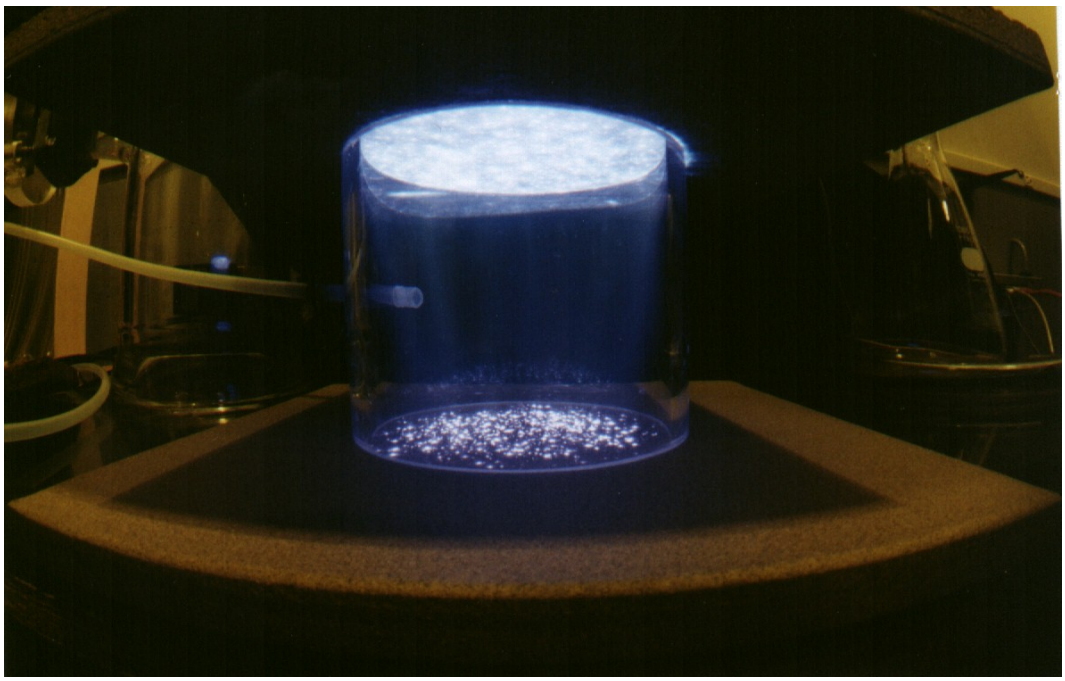

Figure-7.13 Helium discharge photographed by a fish eye camera

CHAPTER 8

Biological Results

The biological phase of this project was designed to demonstrate the effectiveness of ionized gases as a rapid and potent means to decontaminate potential hazardous biological agents including bacteria, viruses, and spores. The foremost objective was to determine the effectiveness of ionized gases on bacteria. Prior to testing the ionized gases on living cells, it was required that the ionized gas generator meet the environmental health and federally mandated safety standards. For the reason that ionized gases is expected to be harmful to bacteria, technical personnel are potentially at risk. Since ozone was known to be a predominant gas during operation, it was necessary to demonstrate that ozone or any other potentially harmful gasses could be removed and technical personnel were not exposed. These criteria were met by demonstrating that when the discharge chamber was placed in a chemical fume hood in the laboratory, the exhaust fan was able to effectively move air from the outside environment through the exhaust vent as determined by using an innocuous smoke.

Bacteria at a dilution that achieved a countable number of colonies per plate (20-80 colonies) were plated onto an agar plate, exposed or not exposed to ionized gases for various periods of time, grown over night in an incubator at 37°C, and counted the next morning to determine the effects of ionized gas treatment. The number of colonies on exposed plates was divided by the number of colonies on unexposed plate and then

multiplied by 100 to determine the percent survival (or percent killing calculated as 1 minus percent survival). The following protocol was used in each experimental trial.

A glycerol stock of XL-1 Blue^{TM} *E. coli* was cultured in 10 ml Luria-Bertani Broth (LB medium) for 24 hours in a shaking incubator (37°C, 220 RPM). The overnight culture was diluted 1x10^{6} in LB medium and the diluted suspension (100 μl) was plated on a LB agar plate. The plate was incubated (37°C) for 24 hours. LB medium (10 ml) was inoculated with a single colony from the overnight cultured plate and incubated in the shaking incubator for 24 hours to get freshly prepared stationary phase *E. coli*. In order to observe the effects of ionized gas effects on the growth rate of *E. coli*, log phase *E. coli* were prepared in the following way.

Freshly prepared stationary phase *E. coli* was diluted 1/10 into LB medium and incubated in the shaking incubator for one and a half hours to let *E. coli* reach log phase with an absorbance at 660nm was near 1.0. The bacteria were diluted to obtain a reading of exactly 1.0 and further diluted 1x10^{6}, plated on agar plates and grown overnight in an incubator at 37°C. When plated on agarose plates and grown overnight, this provided an appropriate number of bacterial colonies to count with and without treatment with ionized gasses (Yu et al., IEEE 2002). Using this design as shown in Figure 8.1 in two trials, bacteria were exposed to ionized gasses for 0, 15, 30, 60, 180, or 600 seconds. The plates were incubated overnight and colonies were counted 15-20 hours later. Table 3 gives the number of colonies, the range and the percent survival with each of the treatments and the control.

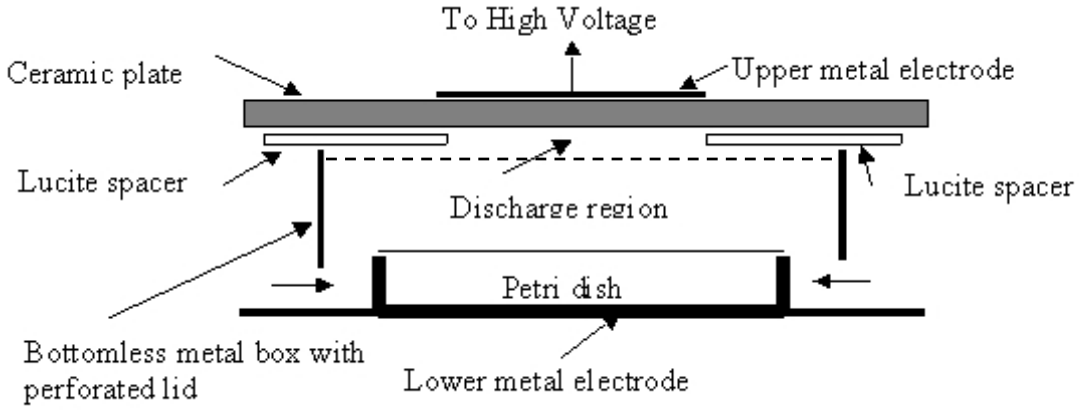

Figure-8.1 The diagram above depicts the initial design of the discharge chamber used for the generation of ionized gasses for the treatment of bacteria and human cells. This unit was incorporated in a larger Plexiglas box with a lid including a safety switch that prevented generation of ionized gasses if the lid was not closed.

Table-3 The number of colonies, the range and the percent survival with each of the treatments and the control.

Time of exposure (seconds)	**Number of colonies/range**	**% Survival**
0	46.0 ± 0	100%
15	39.5 ± 6.4	85%
30	34.5 ± 0.7	75%
60	51.0 ± 22	48%
180	6.0 ± 4.2	13%
600	0.0 ± 0	0%

Figure 8.2 shows the survival curve of the E.Coli bacteria exposed to the plasma discharge. The results indicated that effective killing did not occur until bacteria were exposed to ionized gasses for nearly 3 minutes (180 seconds), when only 13% of the bacteria survived. All bacteria were dead after exposure for 10 minutes (600 seconds). While the ionized gases were effective in killing bacteria, the exposure time was longer than anticipated.Design changes were made in the discharge chamber in an attempt to decrease the exposure time and increase the killing effectiveness. In the model shown in Figure 8.3 requires a closer association between the source of the ionized gasses and the surface to be contaminated, but was anticipated to require shorter exposure times. Because the effectiveness of killing bacteria was not completely adequate, the first design was modified to close the Petri dish more completely by reducing the volume of the discharge chamber as indicated below.

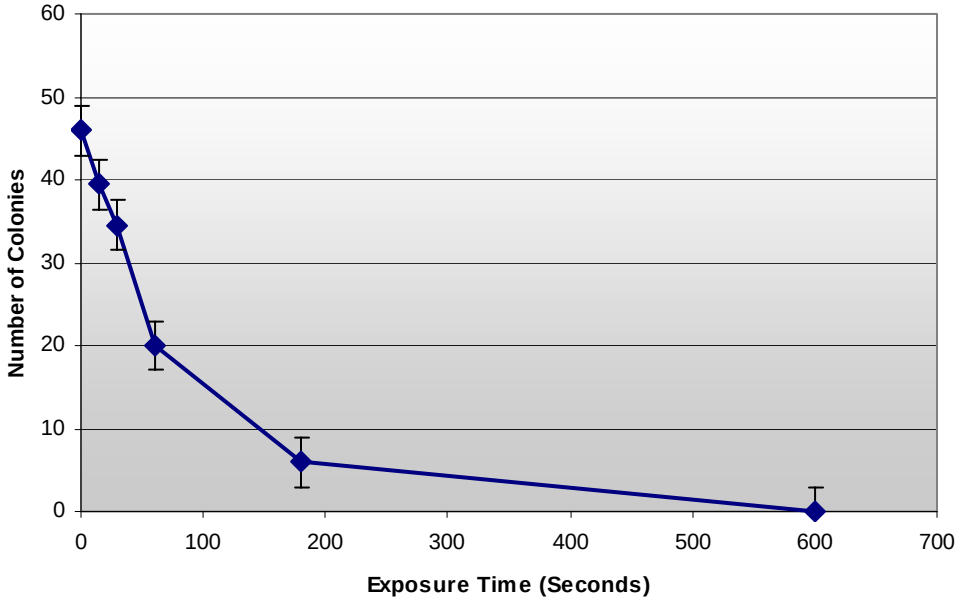

Figure-8.2 Survival curve of E. Coli bacteria exposed to atmospheric pressure plasma discharge.

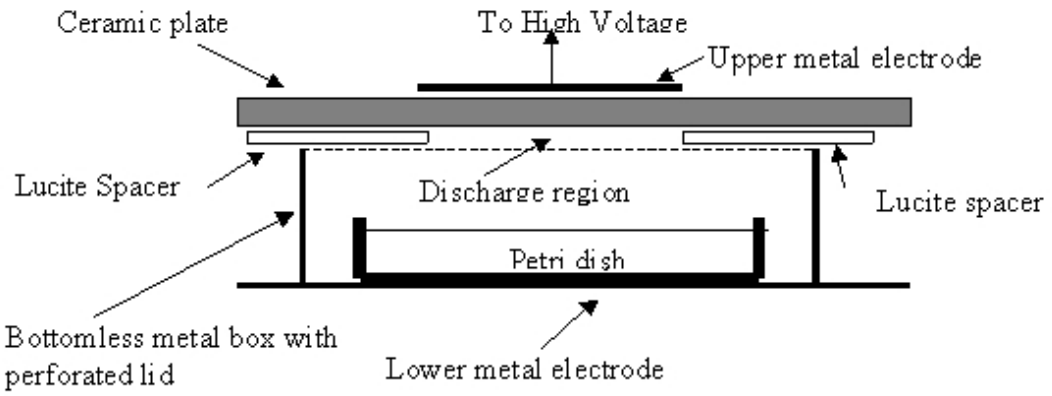

Figure-8.3 The diagram above depicts the modified design of the discharge chamber used for the generation of ionized gasses for the treatment of bacteria and human cells. This unit was incorporated in a larger Plexiglas box with a lid including a safety switch that prevented generation of ionized gasses if the lid was not closed.

Therefore in the next experimental paradigm, the exposure times were decreased in anticipation that the new design would more effectively decontaminate. In three separate trials, bacteria on agar plates were exposed to ionized gasses for 0, 10, 20, 30, 60, and 180 seconds. As before, the control and exposed plates were incubated overnight and colonies were counted 15-20 hour later. The results are shown in Table 4 below. With this improved chamber design, approximately half of the bacteria were killed in 20 seconds and none of the bacteria survived 3 minutes of (180 seconds) of treatment. The improved survival curve of the bacteria exposed to the modified discharge setup is shown in Figure 8.4.

Table-4 The number of colonies, the range and the percent survival with each of the treatments and the control with the improved chamber design.

Time of exposure (seconds)	Number of colonies/range	% survival
0	20 ± 2.0	100%
15	14.6 ± 2.8	73.3%
30	11.0 ± 0.6	55.0%
60	5.7 ± 0.3	28.3%
180	2.0 ± 1.2	10.0%
600	0.0 ± 0	0%

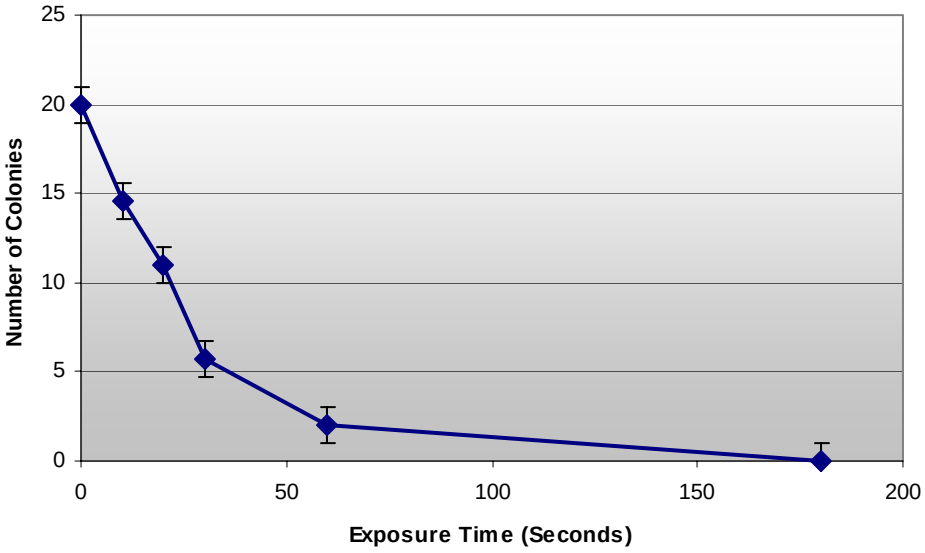

Figure-8.4 Improved Survival curve of E. Coli bacteria exposed to modified atmospheric pressure plasma discharge.

The results of these experiments indicate that effective decontamination can be achieved within minutes, when bacteria are exposed to ionized gases in close contact to the contaminating surface. On the battlefield or in remote locations, ionized gases could be used to decontaminate potentially harmful agents of bacterial origin. In hospitals on the battlefield and/or in remote locations, ionized gasses could be used to sterilize surgical equipment, decontaminate potentially infected areas in post-operative care units following surgery. In such cases the self-generated gas flow from the reactor facilitates the application of the ionized gases over the large infected areas. To check on gas flow produced by a DC discharge, we looked for and observed gas flow produced by a ceramic electrode.

We hypothesized that ionized gases also could have effects for better and/or worse on eukaryotes, including human cells. The potential applications of plasmas in biology and medicine depend on whether they terminate, modulate, or potentate cell function. It is hypothesized that they can do all of these depending on the conditions for plasma generation. The application of ionized gasses on eukaryotic cells has not been investigated. It is possible to apply this technology to probe cell structure and function. Based on information already known, reactive oxygen species and other ions related to stress are known to have effects on cell function. Nitric oxide, a short lived soluble gas, is known to be a factor for communications between cells (a paracrine factor), best characterized for potent relaxation of smooth muscle and in killing reactions in

macrophages. Thus, these endogenous factors serve as potential models for comparison with ionized gasses.

Although these ionized gases from cold plasmas may not have been present during biological evolution they represent pressures that are not unlike others conditions that have shaped evolution during the ages. Thus, information on effects of plasmas on cell function and cell signaling networks will provide valuable new tools to modulate intracellular signaling for a better understanding of how cells function in response to environmental stresses. Knowledge of signal mechanisms could provide new potential target for therapeutic intervention in diseases related to cancer, autoimmunity, and aging/senescence, among others. An understanding of how plasmas may affect respiration, cell cycle, proliferation, and/or apoptosis will provide a greater understanding of these cell functions in general.

In a single trial carried out so far, cold plasmas, when applied to cells covered with minimal amounts of media, reduced the attachment of cells to the cell culture plate. It is not known if this is due to apoptosis, necrosis, or other cell signaling mechanisms. The inappropriate detachment of cells is known to induce a form of apoptosis in normal cells, but not in metastatic cancer cells, called anoikis. Further experiments are in progress to determine the mechanism of cell detachment and to determine if this may serve as a model to study processes of metastasis.

CHAPTER 9

Surface Discharge

The conventional reactor setup is modified to produce surface discharge on the moistened unglazed ceramic barrier. The surface discharge works very well with the resistive barrier discharge. We have constructed ceramic barriers of wide variety of shapes and sizes to test the pliability of the discharge. In the surface discharge the electrodes are in contact with the moistened ceramic material and the discharge formed on the surface of the barrier. The Figure 9.1 shows the schematic representation of the surface barrier discharge.

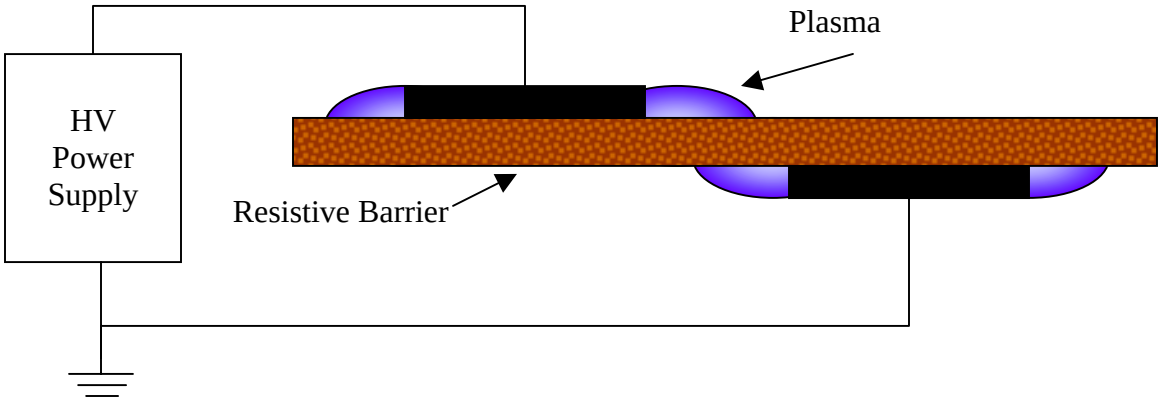

Figure-9.1 The schematic of the basic surface discharge setup

The Figure 9.2 shows the ceramic electrodes of different shapes and sizes tested for the surface discharge. The surface discharge lasts as long as the ceramic barrier has enough moisture. After few minutes of operation the discharge formed on a slab of ceramic begins to arc. In order to solve this problem we have constructed the ceramic materials in the shape of containers to store water. The stored water in the ceramic material keeps it moistened enough for the discharge operation for a long time. The discharge was operated for long time with this arrangement. A series of surface discharge photographs are shown in Figure 9.3. The surface discharge is also tested as an aerodynamic plasma thruster. The experimental setup is very similar to the Figure 9.1. The production of airflow is physically identified by a smoke system. In which the airflow is identified by the smoke traces. The Figure 9.4 shows the intense production of airflow when the discharge is ON.

Figure 9.2 Ceramic electrodes developed for surface discharge

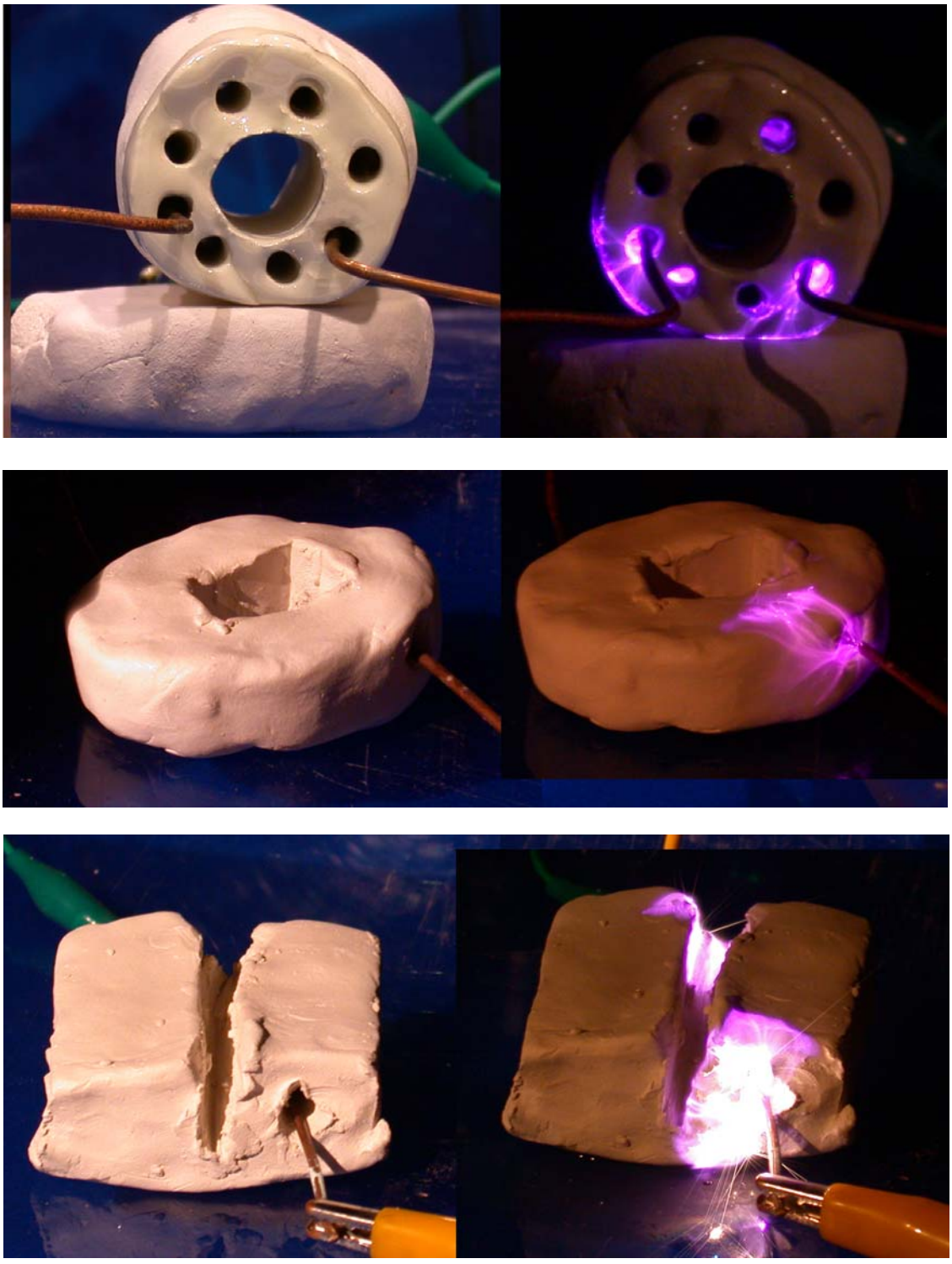

Figure 9.3 Series of resistive barrier surface discharge of different structural shapes.

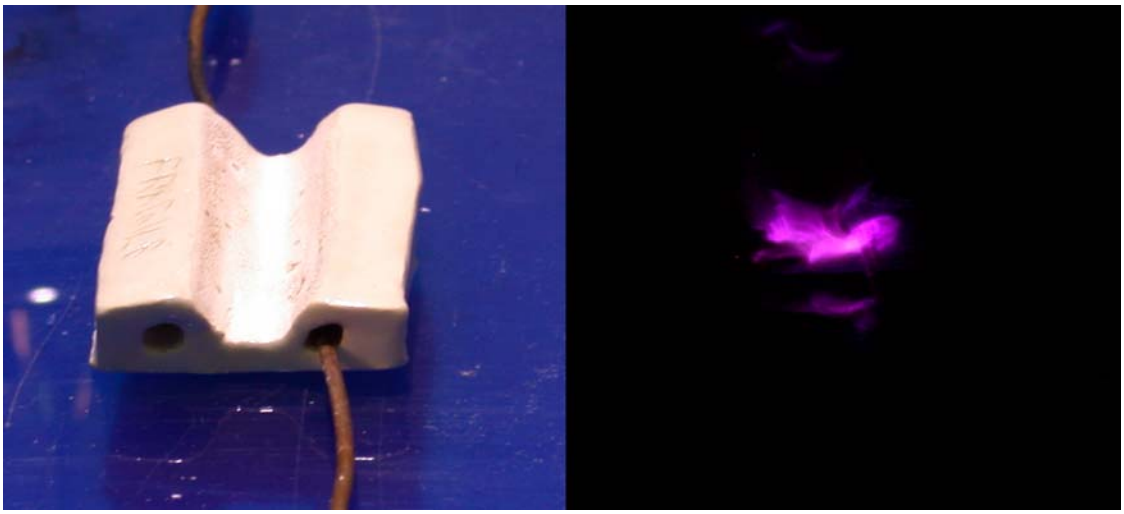

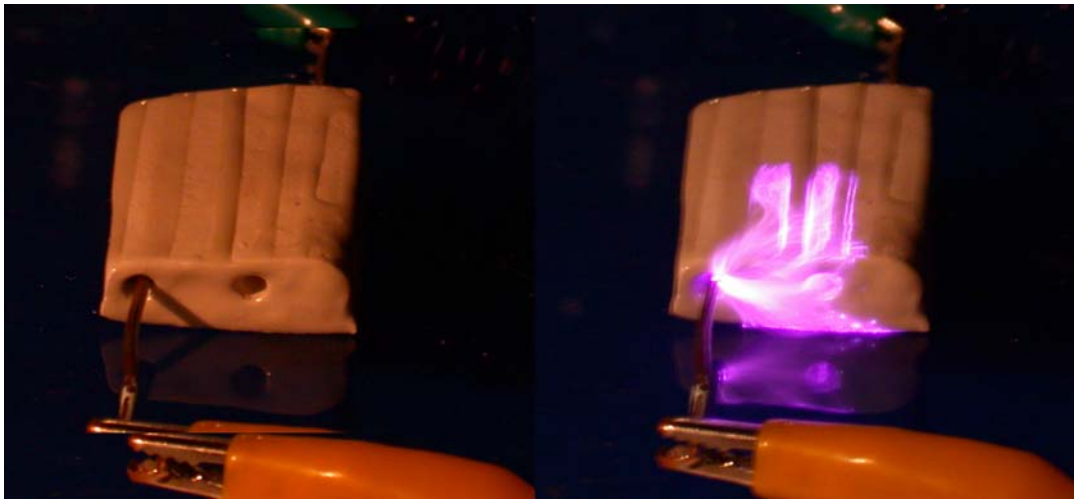

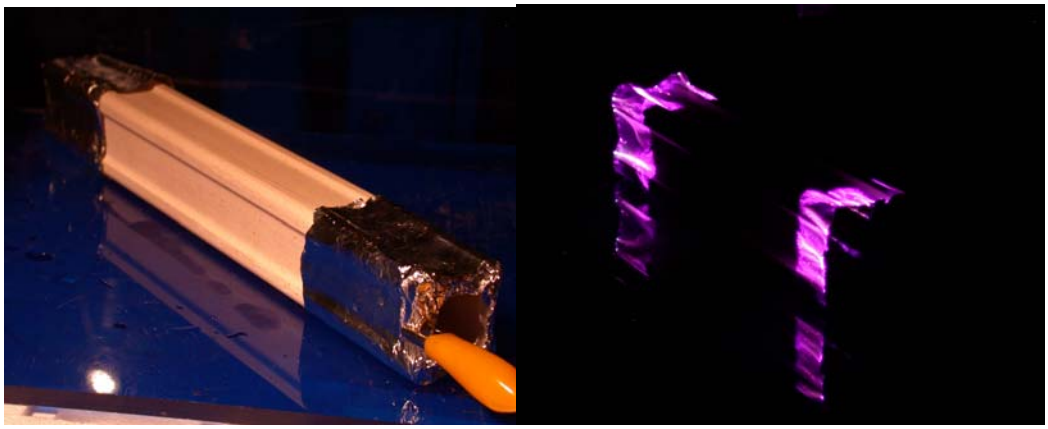

Figure-9.3 Continued

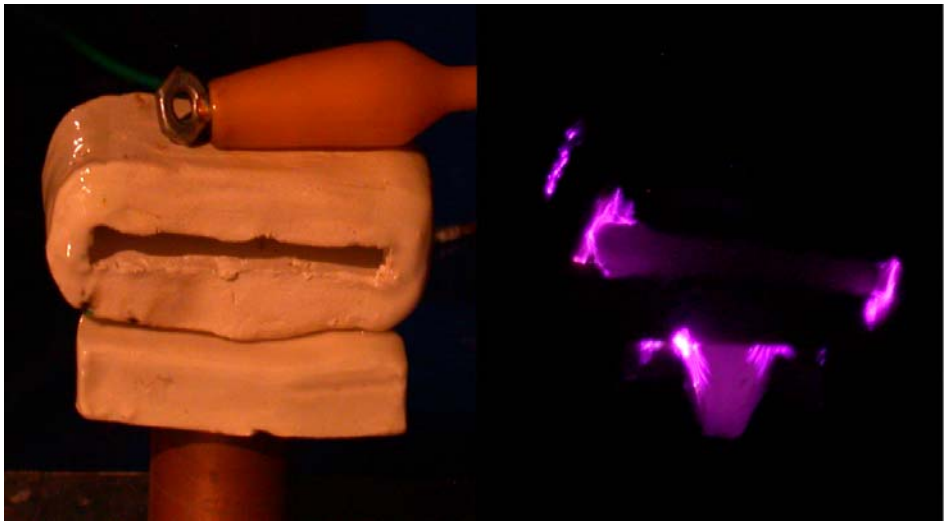

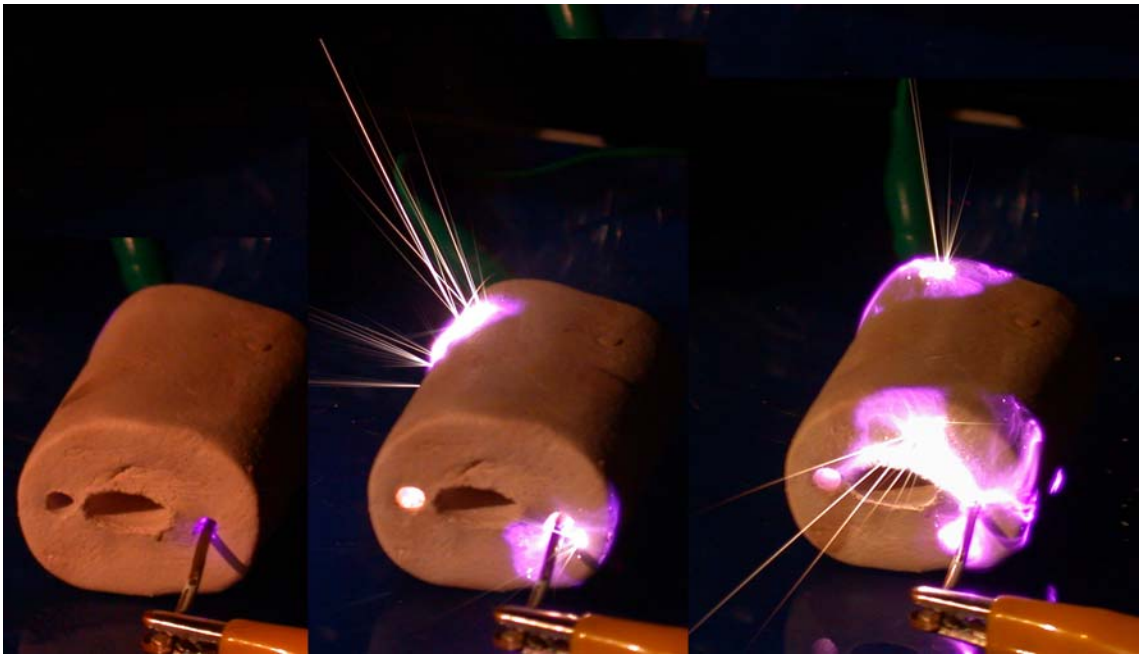

Figure-9.3 Continued

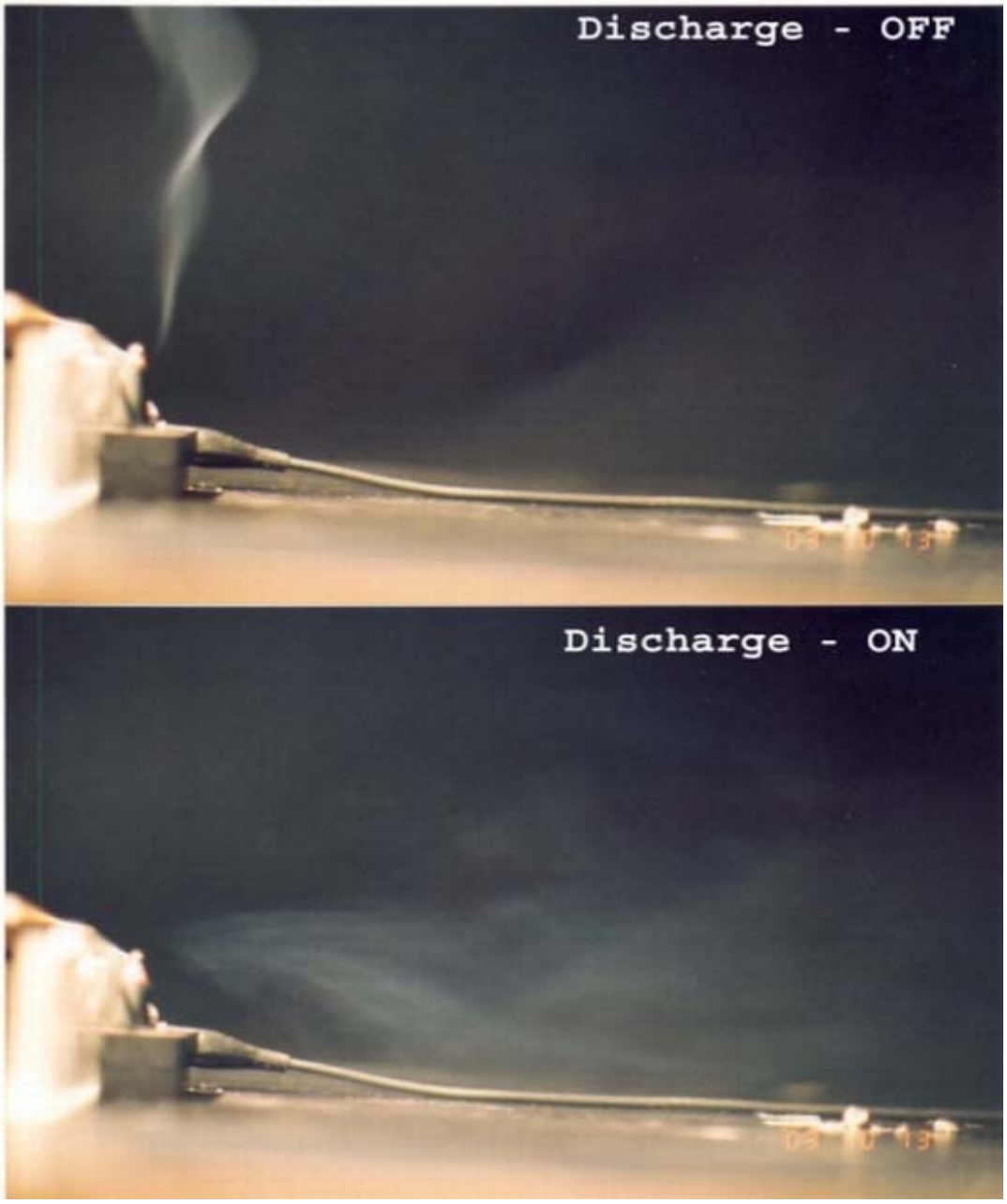

Figure-9.4 Intense self-generated gas flow produced by a ceramic electrode DC discharge.

CHAPTER 10

Discussion

The resistive barrier discharge generates a **Plasma**, a cloud of ionized gas, at atmospheric pressure and low temperature. Plasma has been shown to be extremely effective in destroying bacteria on surfaces and in the air.

The **US Military** is extremely interested in using atmospheric pressure plasma to decontaminate military equipment that has been contaminated during biological warfare. In addition to decontamination, the atmospheric pressure discharge is used for surface modification. For example, nonwoven plastic cloth is normally water repellent. When treated with plasma discharges, the fabric becomes water-absorbent. The plastic cloth also can be permanently electrically charged to attract dust particles. There is at present a wide market for atmospheric pressure plasma discharges. However, the competing research technique uses a dielectric barrier discharge that requires an expensive radio transmitter to produce. The resistive barrier discharge apparatus developed makes the atmospheric pressure plasmas **affordable**.

The developed resistive barrier discharge has many advantages. The first advantage of our technique over the competition of DBD is a reduction in cost of about a factor of 10, because our apparatus does not require a high-power radio transmitter.

The second advantage is that in atmospheric pressure helium, we can make many liters of plasma, while the DBD can only make layers a few millimeters thick.

The third advantage is that electrode material of our technique is essentially water, confined in a porous ceramic. Water produces the OH radical, and biological experiments show that the OH radical is much more effective at sterilization than ozone or atomic oxygen.

This research has a wide variety of applications. It can be used for destroying allergens in homes for people with severe allergy problems, Surface modification of materials, to cause water or paint to stick to plastics, Sterilization of medical instruments -Endoscopes cannot be sterilized with heat, as heat destroys the optics; the present sterilization technique uses poisonous ethylene oxide, and requires several days to take effect.

CHAPTER 11

Conclusion and Prospects

It has been clearly shown that much information can be obtained from the study of steady state atmospheric pressure nonthermal resistive barrier discharge in various gases when multiple simultaneous real time diagnostics are used. It has been clearly shown that the above-mentioned reactor has a tremendous production rate of ozone. It is widely evident that the ozone is one of the prime active species for biological inactivation or decontamination.

The dual mode steady state atmospheric pressure non-thermal resistive barrier discharge is currently being investigated for biological decontamination. The goals of our work are to prepare an effective, inexpensive plasma sterilization process and to identify and escalate the main contributing active species. The resistive barrier discharge produce non – equilibrium plasma at atmospheric pressure, and at room temperature.

The barrier discharge works on two modes with atmospheric air as the working gas. In general it operates in filamentary mode, but under special conditions a diffuse mode can be generated. Diffuse plasma is produced when noble gases such as helium or argon are used. Various active species produced by the discharge have been discussed. The electrical characteristics of the discharge are well explained with its physical parameters.

The discharge has a tremendous production rate of ozone, which is considered to be the prime factor for effective biological sterilization. In addition, it is highly believed that ions and molecular fragments may also sterilize items causing both decontamination and surface modification. The production cost of this plasma reactor is very less when compared to one atmospheric plasma reactors which requires expensive high voltage RF power supplies for its operation. The reactor, which is designed, works on both AC and DC. It is considered to be an advantage of flexibility of its operation especially in distant and/or isolated locations. The running cost and the maintenance cost is far less compared to other conventional plasma reactors. The production, running, and maintenance costs are important factors when the decontamination is concerned with large area applications such as during widespread attacks involving chemical or biological warfare (CBW) agents.

The future steps of our investigation on the principle mechanisms will be the further studies of biological deactivation by testing wide variety of biological samples and samples of chemical warfare agents. The modification of the reactor system suitable for surface discharge and its applications is also concerned. It is strongly believed that substantial improvements in the rate of decontamination can be achieved by further improvements to the design plasma reactor chamber and the use of various diagnostic measurements for the active species measurements. To this belongs the qualitative and quantitative measurements of ultraviolet light emission and measurement of atomic oxygen (O), meta stable oxygen (O_2*) and oxygen ions (O_2^+). The production of atomic

oxygen can be utilized to generate Nitrogen oxides as well as oxidation of other chemical reactive components.

REFERENCES

Bithell, R.M., 1982. Package and sterilizing process for same. US Patent 4 321 232.

Block, S.S., 1991. Peroxygen compounds. In: Block, S.S. (Ed.), Disinfection, Sterilization, and Preservation, 4th edn. Lea and Febiger, London Chap. 9.

Boucher (Gut), R.M., 1980. Seeded gas plasma sterilization method. US Patent 4 207.

Boucher (Gut), R.M., 1985. State of the art in gas plasma sterilization. Med. Device Diagnost. Indust. 7, 51–56.

Brandenburg R, Kozlov KV, Gherardi N, Michel P, Khampan C, Wagner H-E, Massines F. Proceedings of the Eighth International Symposium on High Pressure, Low Temperature Plasma Chemistry, HAKONE VIII, P. uhaj- .arve (Estonia), 2002. p. 28.

Braun D, K.uchler U, Pietsch GJ. J Phys D: Appl Phys 1991;24:564.

Cariou-Travers, S., Darbord, J.C., 2001. Validation biologique de ste´rilisation plasma: cas du Sterrad®. Le Vide: Sci. Tech. Applic. 299, 34–46.

Delcroix, J.-L., Bers, A., 1994. Physique des Plasmas (Chap. I). InterE´ ditions/CNRS E´ dition, Paris.

Donohoe KG. PhD thesis, California Institute of Technology, Pasadena, CA, 1976.

Ehrenberg, L., Hiesche, K.D., Osterman-Golkar, S., Wenneberg, I., 1974. Evaluation of genetic risks of alkylating agents. Mutat. Res. 24, 83–103.

Eliasson B, Hirth M, Kogelschatz U. J Phys D: Appl Phys 1987;20:1421.

Eliasson B, Kogelschatz U. IEEE Trans Plasma Sci 1991;19(2):309;

Ernest, A., 1995. Why hospitals are adopting new sterilization technologies. 1, 1–3.

Gherardi N, Gouda G, Gat E, Ricard A, Massines F. Plasma Sources Sci Technol 2000;9:340.

Gibalov VI, Pietsch GJ. J Phys D: Appl Phys 2000; 33:2618.

Gibalov VI, Pietsch GJ. J Phys D: Appl Phys 2000; 33:2618.

Golubovski Yu B, Maiorov A, Behnke J, Behnke JF. Proceedings of the Eighth International Symposium on High Pressure, Low Temperature Plasma Chemistry, HAKONE VIII, P.uhaj.arve (Estonia), 2002. p. 48, 53.

Griffiths, C.N., Raybone, D., 1992. Gas sterilization. PCT (Patent) WO 92/15336.

H.B. Dixon, “On Conditions of Chemical Change in Gases,” *Phil. Trans. Royal Soc.*, vol. 175, pp. 617, 1884.

Henn, G.G., Birkinshaw, C., Buggy, M., Jones, E., 1996. A comparison study of the effects of gamma-irradiation and ethylene oxide sterilization on the properties of compression moulded poly-D-L-lactide. J. Mat. Sci.—Mater. Med. 7, 591–595.

Holyoak, G.R., Wang, S., Liu, Y., Bunch, T.D., 1996. Toxic effects of ethylene oxide residues on bovine embryos in vitro. Toxicology 108, 33–38.

I. Alexeff, W. D. Jones, K. Lonngren, D. Montgomery, "Transient Plasma Sheath Discovered by Ion Acoustic Waves", *Physics of Fluids,* vol-12, pp-345-346, Feb 1969

I. Alexeff, M. Laroussi, W. Kang, and C. Malott, “Biological applications of nonequilibrium plasmas,” in *Proc. Int. Symp. Non-Thermal Medical/Biological Treatments Using EM Fields and Ionised Gases,* Norfolk, VA, 1999, p. 110.

I. Alexeff, “Direct Current Energy Discharge System,” U.S.Patent 6232732, 05/15/2001.

I. Alexeff, M. Laroussi, "The Uniform, Steady-State Atmospheric Pressure DC Plasma", *IEEE Trans. Plasma Sci.*, vol. 30. pp. 174-175, Feb. 2002.

I. Alexeff, S. Parameswaran, M. Thiyagarajan, "Characteristics of the steady-state atmospheric pressure DC discharge", *Plasma Science*, 2003. ICOPS 2003. IEEE Conference Record, pp. 298.

James Dillon Cobine, “Gaseous Conductors - Theory and Engineering Applications”, Book, sec. 4.9.

Kanazawa S, Kogoma M, Moriwaki T, Okazaki S. International Symposium on Plasma Chemistry, Tokyo (Japan), 1987. p. 1844.

Kanazawa S, Kogoma M, Moriwaki T, Okazaki S. J Phys D: Appl Phys 1988;21:838.

Kelly-Wintenberg, K., Montie, T.C., Brickman, C., Roth, J.R., Carr, A.K., Sorge, K., et al., 1998. Room temperature sterilization of surfaces and fabrics with a one atmosphere uniform glow discharge plasma. J. Indust. Microbiol. Biotechnol. 20, 69–74.

Khomich, V.A., Soloshenko, I.A., Tsiolko, V.V., Mikhno, I.L., 1997. Cold sterilization of medical devices and materials by plasma DC glow discharge. In: Proceedings of the 12th International Conference on Gas Discharge and their Applications, Greifswald, vol. 2, pp. 740–744.

Kogelschatz U, Salge J. High-pressure plasmas: dielectricbarrier and corona discharges properties and technical applications. In: Pfau S, Schmidt M, Hippler R, Schoenbach KH, editors. Lectures on plasma physics and plasma technology. Weinheim/Germany: Wiley Verlag Chemie, 2001. p. 305.

Kozlov KV, Wagner H-E, Brandenburg R, Michel P. J Phys D: Appl Phys 2001;34:3164.

Krebs, M.C., Be´casse, P., Verjat, D., Darbord, J.C., 1998. Gas plasma sterilization: relative efficacy of the hydrogen peroxide phase compared with that of the plasma phase. Int. J. Pharmac. 160, 75–81.

Kuzmichev, A.I., Soloshenko, I.A., Tsiolko, V.V., Kryzhanovsky, V.I., Bazhenov, V. Yu, Mikhno, I.L., et al., 2000. Features of sterilization by different types of atmospheric-pressure discharges. In: Proceedings of the International Symposium on High Pressure

L. A. Rosocha, G. K. Anderson, L. A. Bechtold, J. J. Coogan, H. G. Heck, M. Kang, W. H. McCulla, R. A. Tennant, and P. J. Wantuck, “Treatment of hazardous organic wastes using silent discharge plasmas,” *in Non-Thermal Plasma Techniques for Pollution Control: Part B,* ser. NATO ASI series. Germany: Springer-Verlag, pp. 281-308, 1993,

Laroussi, M.; Alexeff, I.; Kang, W.L., 2000, "Biological decontamination by nonthermal plasmas", IEEE Trans. Plasma Sci., Vol 28 , No. 1 , Feb. 2000, pp 184 – 188.

Lerouge, S., Fozza, A.C., Wertheimer, M.R., Marchand, R., Yahia, L’H., 2000a. Sterilization by low-pressure plasma: the role of vacuum-ultraviolet radiation. Plasmas and Polymers 5, 31–46.

Lerouge, S., Wertheimer, M.R., Marchand, R., Tabrizian, M., Yahia, L.H., 2000b. Effect of gas composition on spore mortality during low-pressure plasma sterilization. J. Biomed. Mater. Res. 51, 128–135.

Low Temperature Plasma Chemistry (HAKONE VII), Greifswald, Germany, vol. 2, pp. 402–406.

M. A. Tas, R. van Hardeveld, and E. M. van Veldhuizen, “Reactions of NO in a positive streamer corona plasma,” *Plasma Chem. Plasma Proc.*, vol. 17, no. 4, pp. 371-391, 1997.

Marcos-Martin, M.-A., Bardat, A., Schmitthaeusler, R., Beysens, D., 1996. Sterilization by vapour condensation. Pharm. Techn. Eur. 8, 24–32.

Massines F, Mayoux C, Messaoudi R, Rabehi A, Segur P. International Conference on Gas Discharges and Their Applications, Swansea (UK), 1992. p. 730.

Massines F, Messaoudi R, Mayoux C. Plasmas Polym 1998;(3):43.
Massines F, Rabehi A, Decomps P, Ben Gadri R, Segur P, Mayoux C. J Appl Phys 1998;83:2950.

Massines F, Gherardi N, Sommer F. Plasmas Polym 2000;5(3):151.

Menashi, W.P., 1968. Treatment of surfaces. US Patent 3 383 163.

M. Laroussi, “Sterilization of contaminated matter with an atmospheric-pressure plasma.” *IEEE Trans. Plasma Sci.*, vol. 24, pp. 1188-1191, June 1996.

M. Laroussi, I. Alexeff, W. Kang, “Biological Decontamination by Non-Thermal Plasmas,” *IEEE Trans. Plasma Sci.*, vol. 28, pp. 184 – 188. Feb. 2000.

Moats, W.A., 1971. Kinetics of thermal death of bacteria. J. Bacteriol. 105, 165–171.

Moisan, M., Pelletier, J., 1999. Microwave Excited Plasmas. Elsevier, Amsterdam.

Moreau, S., Moisan, M., Tabrizian, M., Barbeau, J., Pelletier, J., Ricard, A., et al., 2000. Using the flowing afterglow of a plasma to inactivate Bacillus subtilis spores: influence of the operating conditions. J. Appl. Phys. 88, 1166–1174.

Morris, J.C., 1970. Disinfectant chemistry and biocidal activities. In: Proceedings of the National Specialty Conference in Disinfection, New York.

M. Rader, I. Alexeff, L. Wadsworth, “A summary of available commercial atmospheric radio-frequency plasma processing equipment for surface microfication of melt-blown and spun bond plastic cloth,” *IEEE International conference on Plasma Science*, 3-5 June 1996, pp. 148

M. Thiyagarajan, I. Alexeff, S. Parameswaran, S. Beebe, "A Dual Mode Steady State Atmospheric Pressure Non Thermal Resistive Barrier Plasma Discharge For Biological Decontamination: Electrical, Chemical, Optical and Biological Studies", *Bulletin of the American Physical Society*, vol. 48, No. 6.

Okazaki S, Kogoma M, Uehara M, Kimura Y. J Phys D: Appl Phys 1993;26:889.

Peeples, R.E., Anderson, N.R., 1985a. Microwave coupled plasma sterilization and depyrogenation I. System characteristics. J. Parent. Sci. Technol. 39, 2–8.

Pflug, I.J., Holcomb, R.G., 1991. Principles of the thermal destruction of microorganisms. In: Block, S.S. (Ed.), Disinfection, Sterilization, and Preservation, 4th edn. Lea and Febiger, London Chap. 6.

Pietsch GJ. Contrib Plasma Phys 2001;41(6):620.

Pons, M., Pelletier, J., Joubert, O., 1994. Anisotropic etching of polymers in SO2/O2 plasmas: hypotheses on surface mechanisms. J. Appl. Phys. 75, 4709–4715.

R. A. Roush, R. K. Hutcherson, M. W. Ingram, and M. G. Grothaus, “Effects of pulse risetime and pulsewidth on the destruction of toluene and NO_x in a coaxial pulsed corona reactor,” in *Proc. 22nd Int. Power Modulator Symp.*, Boca Raton, FL, pp. 79-84., June 25-27, 1996.

Samoilovich V, Gibalov V, Kozlov K. Physical chemistry of the barrier discharge. D. usseldorf: DVS-Verlag GmbH, 1997.

Sawada Y, Ogawa S, Kogoma M. J Phys D: Appl Phys 1995;28:1661.

Segur P, Massines F. Proceedings of the International Conference on Gas Discharges and Their Applications, Glasgow (UK), 2000. p. 15.

Steelman, V.M., 1992a. Ethylene oxide: the importance of aeration. Aorn J. 55, 773–787.

Steelman, V.M., 1992b. Issues in sterilization and disinfection. Urol. Nurs. 12, 123–127.

Tensmeyer, L.G., Wright, P.E., Fegenbush, D.O., Snapp, S.W., 1981. Sterilization of glass containers by laser initiated plasmas. J. Parent. Sci. Technol. 35, 93–96.

Trunec D, Brablec A, Stastny F. Contrib Plasma Phys 1998;38:435.
Tepper J, Lindmayer M, Salge J. Proceedings of the Sixth International Symposium on High Pressure Low Temperature Plasma Chemistry, HAKONE VI, Cork (Ireland), 1998. p. 123.

Trunec D, Brandenburg R, Michel P, Pasedag D, Wagner H-E, Navratil Z. Proceedings of the International Symposium on High Pressure, Low Temperature Plasma Chemistry, HAKONE VIII, P.uhaj.arve (Estonia), 2002. p. 63.

V. A. Godyak, N. Sternberg, “Smooth Plasma-Sheath Transition in a Hydrodynamic Model”, *IEEE Trans. Plasma Sci.*, vol. 18, pp. 159-168, Feb 1990.

Wagner H-E, Brandenburg R, Michel P, Massines F, Kozlov KV. Proceedings of the seventh International Symposium on High Pressure Low Temperature Plasma Chemistry, HAKONE VII, Greifswald (Germany), 2000. p. 93.

Wertheimer, M.R., Fozza, A.C., Holla¨nder, A., 1999. Industrial processing of polymers by low-pressure plasmas: the role of VUV radiation. Nucl. Inst. Meth. Sect. B 151, 65–75.

Zhang, Y.-Z., Bjursten, L.M., Freij-Larson, C., Kober, M., Wessle´n, B., 1996. Tissue response to commercial silicone and polyurethane elastomers after different sterilization procedures. Biomaterials 17, 2265–2272.

Zakrzewski, Z., Moisan, M., 1995. Plasma sources using long linear microwave field applicators: main features, classification and modelling. Plasma Sources Sci. Technol. 4, 379–397.

VITA

Magesh Thiyagarajan was born in Chennai, India. He received the Bachelor of Engineering degree in Electrical and Electronics Engineering from the University of Madras, India in 2001. He received the prestigious Medal of Honor from the University of Madras for excellence in academic work during his undergraduate studies.

In August 2002, he began pursuit of a Master of Science degree in the Department of Electrical & Computer Engineering at the University of Tennessee, Knoxville. There he has served as a Graduate Research Assistant from 2002 to 2004. He has six recent publications in his area of research.

He has been awarded the prestigious University of Tennessee Citation Award for Extraordinary Professional Promise for the year 2004. He is a student member of the IEEE and a member of the electrical engineering honor society Eta Kappa Nu and the engineering honor society Tau Beta Pi.

He has been offered to pursue the Doctorate degree in Electrical Engineering at the University of Wisconsin – Madison, beginning summer 2004.